

Revised Multiple Replication 60802 Time Domain Simulation Results for Cases with Drift Tracking Algorithms and PLL Noise Generation

Version 0

Geoffrey M. Garner
Analog Devices (Consultant)

gmgarner@alum.mit.edu

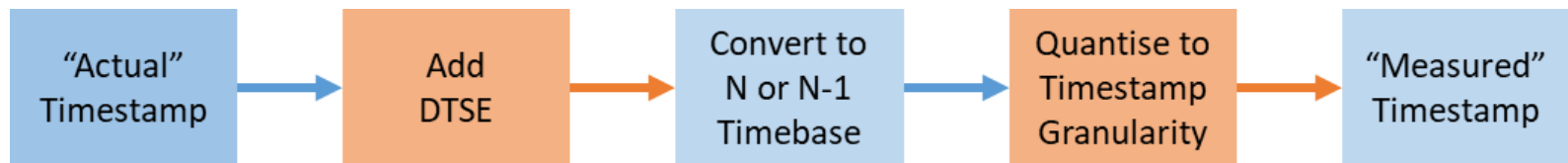
IEEE 802.1 TSN TG
2024.05.13

New Introduction (Preface)

- This presentation contains a major revision of the assumptions and results for the time-domain simulations of [13] for accumulated maximum absolute value of time error over 100 hops (101 nodes)
- While the presentation can be considered a revision of [13], there is a large amount of new or revised content
 - As a result, it is considered a new presentation
 - However, most of the background material is taken from [13]
- The following slides summarize the new or revised assumptions, compared to the assumptions of [13]
 - Much of this material is copied from [14]
- The remainder of the presentation follows [13]
 - Much of the material is copied from [13], with revisions where needed; this includes the revised assumptions and the new simulation results

Revised Assumptions Relative to [11] - 1

- ❑ The Pdelay interval is assumed uniformly distributed in the range [119 ms, 131 ms] (same as Sync Interval)
- ❑ Dynamic timestamp error is added before computing the effect of timestamp granularity, rather than after (see figure below, supplied by [12])



- ❑ While endpoint filter noise generation was modeled in the simulator for the analyses of [13], it was accidentally not turned on in those analyses
 - In the current presentation, simulations both with and without endpoint filter noise generation were run for each case
- ❑ The IIR filter for mean link delay uses coefficients $a_1 = 0.999$, and $b_0 = 0.001$ (rather than 0.99 and 0.01)
- ❑ The upper bound of the pdelay turnaround time distribution is 15 ms (it was mistakenly set to 1.5 ms in [13])

Revised Assumptions Relative to [11] - 3

- When computing TSGE, $\frac{1}{2}$ of the timestamp granularity is added after the truncation for all timestamps at all nodes, rather than only at the GM, as was previously done
 - This change was needed for [14] because TSGE was not the same at all nodes in the analyses there; TSGE was set to zero for some messages at some ports but not at other ports
 - As a result, the $\frac{1}{2}$ of timestamp granularity at successive nodes (other than the GM) did not cancel
 - In the analyses in the current presentation, TSGE is the same at all nodes; however, adding $\frac{1}{2}$ of timestamp granularity for each timestamp of each port of each node does not result in any error

Revised Assumptions Relative to [11] - 3

- When computing the effect of random variation in Sync interval, Pdelay interval, residence time, and pdelay turnaround time, the random variation is assumed to be relative to the ideal simulator clock rather than the local clock
 - Previously, these random variations were assumed to be relative to the local clock, and an approximate model was used to convert them to the ideal clock timebase (see 11.2.1 of [8] for description of this model)
 - The effect of TSGE caused the jumps that were seen in computed unfiltered mean path delay; with this revised assumption, the jumps are eliminated

Introduction - 1

- Recent time sync work in 60802 has focused on developing clock drift tracking and compensation algorithms that would enable the objective of $1 \mu\text{s}$ maximum absolute value of time error relative to the grandmaster PTP Instance ($\max|TE_R|$) to be met over 64 hops, and over 100 hops if possible
- The algorithms are described in [1], and extensive Monte Carlo simulations are documented in [2] and in references cited in [1] and [2] (and in references cited in those references)
- Initial time-domain simulation results, based on single replications of various simulation cases, are given in [10]
 - Time domain simulations are needed because they more precisely model the time-dependent effects present in the algorithms
 - Time domain simulations also model endpoint filtering (e.g., PLL filtering) and noise generation at these filters (the Monte Carlo simulations do not model these effects)
 - The Monte Carlo simulations were used to develop the algorithms because they run several orders of magnitude faster than the time-domain simulations

Introduction - 2

□ The single-replication simulation cases in [10] included

- The drift tracking and compensation algorithms described in [1]
- Endpoint filter (e.g., PLL) noise generation, based on the stated assumptions for local clock stability (i.e., frequency drift behavior for the assumed oscillator type and temperature profile
 - Various PLL filter 3dB bandwidths are considered

□ Note that while the objective for $\max|TE_R|$ is 1 μs , the budget for relative dynamic time error (dTE_R) is 500 ns

- Reference [3] indicates 600 ns budget for dTE_R ; however, it was indicated that 100 ns of this is budgeted for the end application
- This is relevant because the simulations model dTE_R for the network transport, i.e., they do not model constant time error (cTE) nor the error in the end application
- Therefore, this presentation takes 500 ns as the objective for $\max|dTE_R|$

Introduction - 3

- The results in [10] indicate that the $\max|dTE_R|$ objective of 500 ns over 100 hops can be met with:
 - the drift compensation and tracking, and mNRR smoothing, algorithms described in [1]
 - Endpoint filter 3dB bandwidth and gain peaking of 1.8 Hz and 2.1985 dB, respectively
 - Temperature profile, XO frequency stability, and other system parameters as described earlier (with the GM frequency stability equal to one-half the frequency stability at other PTP Instances)
- The results in [10] also suggest that the $\max|dTE_R|$ objective can be met with narrower endpoint filter bandwidth, e.g., 1.5 Hz or 1 Hz
- Since it is necessary to run multiple replications of the simulation cases of interest, to obtain confidence intervals for the 0.95 quantile of $\max|dTE_R|$ and also the maximum, it was decided to run multiple replications of simulations for various endpoint filter bandwidths of 1.5 Hz and less

Introduction - 4

- ❑ The following slides, mostly taken from or adapted from [10], summarize the assumptions for the simulation cases (these assumptions were taken from slides 66 to 74 of [2])
 - Except for the specific endpoint filter bandwidths, the assumptions are the same as for the single-replication cases of [10]
- ❑ The third major bullet item of slide 68 of [2] documented 3 sets of assumptions for the drift tracking and error compensation algorithms
 - These will be described later; however, it was decided that all the multiple replication simulations should use the first set of assumptions
- ❑ The effect of endpoint filter noise generation is modeled as described in [10] and summarized here later
- ❑ The summary of assumptions is followed by a summary of the simulation cases, simulation results, and conclusions

Temperature Profile - 1

- The temperature profile of [2] is a half-sinusoid with dwell time; it is similar to the temperature profile of [4], except that the periods of the sinusoidal increase and decrease are 95 s instead of 125 s
 - The temperature history is assumed to vary between -40°C and $+85^{\circ}\text{C}$, as a half sinusoid over 95 s
 - The dwell times are still 30 s, which means that the period of the temperature variation is 250 s instead of 310 s

Temperature Profile - 2

□ The variation for the initial increase in the first cycle is therefore

$$T(t) = -A \cos(\omega t + \phi) + B$$

where

T = temperature in deg C

t = time in s

$A = 62.5$ deg C

$B = 22.5$ deg C

$$\omega = \frac{2\pi}{190 \text{ s}} = \frac{\pi}{95} \text{ rad/s}$$

$$\phi = \text{phase of the temperature variation (in rad)} = \frac{(\text{phase in s})\pi}{250 \text{ s}} \text{ rad}$$

□ The variation for the subsequent decrease in the first cycle is

$$T(t) = B + A \cos[\omega(t - 125) + \phi]$$

Frequency Stability due to Temperature Variation - 1

- The dependence of frequency offset on temperature is assumed to be as described in [4] and [5] of Reference [5] here and in Reference [6] here
 - Specifically, the values a_0 , a_1 , a_2 , and a_3 computed in [5] of Reference [5] will be used in the cubic polynomial fit, and the resulting frequency offset will be multiplied by 1.1 (i.e., a margin of 10% will be used).
- The frequency stability data that this polynomial fit is based on is contained in the Excel spreadsheet attached to [4] of Reference [5] here
 - This data was provided by the author of [4] of Reference [5] here
- The time variation of frequency offset is obtained from the cubic polynomial frequency dependence on temperature, and the temperature dependence on time described in the previous slide
 - The time variation of phase/time error at the LocalClock entity is obtained by integrating the above frequency versus time waveform
 - The time variation of frequency drift rate at the LocalClock entity is obtained by differentiating the above frequency versus time waveform

Frequency Stability due to Temperature Variation - 2

- ❑ The above gives the frequency stability for non-GM PTP Instances, as indicated slide 68 of [2]
- ❑ For the GM, the frequency offset at a given temperature is one-half the frequency offset at the same temperature for non-GM PTP Instances, i.e., the coefficients a_0 , a_1 , a_2 , and a_3 should be multiplied by 0.5 for the GM (after being increased by the factor of 1.1)
- ❑ The phase offset, frequency offset, and frequency drift rate time history plots given in [4] show the qualitative form of the plots; the only difference here is that the period is 250 s instead of 310 s

Assumptions on Relative Time Offsets of Phase Error Histories at Each Node

- The phase of the LocalClock time error waveform at each node is chosen randomly in the range $[0, T]$, at initialization, where T is the period of the phase and frequency variation waveforms (i.e., 250 s)

Other Assumptions - 1

- ❑ Some of these slides documenting Other Assumptions are adapted from [2]
- ❑ The timestamp granularity is assumed to be 8 ns, based on a 125 MHz clock
 - The timestamp is truncated to the next lower multiple of 8 ns
 - At all nodes, 4 ns is added to each timestamp
- ❑ The dynamic timestamp error is assumed to be uniformly distributed over [-6 ns, +6 ns], and is added prior to the truncation due to timestamp granularity error (TSGE)
- ❑ When GM noise is modeled, interpolation is used to compute dTE_R (relative to the GM), because the dTE samples at the GM and at subsequent PTP Instances are not necessarily computed at the same time
- ❑ The simulation time is 1850 s, with the first 500 s discarded when computing $\max|dTE_R|$ to eliminate the effect of any startup transient
- ❑ 300 multiple replications of each simulation case are run
 - A 99% confidence interval for the 0.95 quantile of $\max|dTE_R|$ is obtained by placing the 300 results in ascending order; the interval extends from the 275th smallest to 294th smallest value, and a point estimate is taken as the 285th smallest value

Other Assumptions - 2

□ Pdelay Interval

- Pdelay is used only to compute meanLinkDelay, and not neighborRateRatio (NRR)
- NRR is computed using successive Sync message (using the syncEgressTimestamp)
- The average Pdelay interval is 125 ms
- The actual Pdelay interval is assumed to be uniformly distributed in the range [119 ms, 131 ms]

□ Sync Interval

- The Sync interval is assumed to be uniformly distributed in the range [119 ms, 131 ms]

□ Residence time

- The residence time is assumed to be a truncated normal distribution with mean of 5 ms and standard deviation of 1.8 ms, truncated at 1 ms and 15 ms
- Probability mass greater than 15 ms and less than 1 ms is assumed to be concentrated at 15 ms and 1 ms, respectively (i.e., truncated values are converted to 15 ms or 1 ms, respectively)

Other Assumptions - 3

□ Pdelay Turnaround Time

- The Pdelay turnaround time is assumed to be a truncated normal distribution with mean of 10 ms and standard deviation of 1.8 ms, truncated at 1 ms and 15 ms
- Probability mass greater than 15 ms and less than 1 ms is assumed to be concentrated at 15 ms and 1 ms, respectively (i.e., truncated values are converted to 15 ms or 1 ms, respectively)

□ Link Delay

- Link delay is assumed to be uniformly distributed between 5 ns and 500 ns
- Link delays are generated randomly at initialization and kept at those values for the entire simulation
- Link asymmetry is not modeled

Other Assumptions - 4

□ Mean Link Delay Averaging

- The averaging function is assumed to be an IIR filter that uses 0.99 of the previously computed value and 0.01 of the most recent measurement
- This is equivalent to the filter of the NOTE of B.4 of 802.1AS-2020, taken as a first-order filter, i.e.,

$$y_k = a_1 y_{k-1} + b_0 x_k$$

- where y_k is the k^{th} filter output, x_k is the k^{th} measurement, $a_1 = 0.999$, and $b_0 = 0.001$

Other Assumptions - 5

- When computing the effect of random variation in Sync interval, Pdelay interval, residence time, and pdelay turnaround time, the random variation is assumed to be relative to the ideal simulator clock rather than the local clock
 - Previously, these random variations were assumed to be relative to the local clock, and an approximate model was used to convert them to the ideal clock timebase (see 11.2.1 of [6] for description of this model)
 - The effect of TSGE caused the jumps that were seen in computed unfiltered mean path delay in [15]; with this revised assumption, the jumps were subsequently eliminated in [14]

Endpoint filter (PLL) Parameters - 1

- ❑ In previous simulations (i.e., prior to the simulations of [10], [13], and the simulation cases here), the following were used for the endpoint PLL parameters K_p (proportional gain), K_i (integral gain), K_o (VCO/DCO gain):
 - $K_p K_o = 11$, $K_i K_o = 65$
- ❑ This corresponds to the following 3dB bandwidth (f_{3dB}), gain peaking, and damping ratio (ζ)
 - $f_{3dB} = 2.5998$ Hz, 2.1985 dB gain peaking, $\zeta = 0.68219$
- ❑ In addition, VCO/DCO noise generation was neglected
- ❑ The PLL model used in the simulator is second-order and linear, with 20 dB/decade roll-off
 - It is based on a discretization that uses an analytically exact integrating factor to integrate the second-order system
 - As a result, the PLL model in the simulator is stable regardless of the time step, i.e., sampling rate (though aliasing of the input or noise is possible)
 - Details are given in Appendix VIII.2.2 of [7] (except that the relation between gain peaking and damping ratio is based on the exact result in 8.2.3 of [8] (see Eqs. (8-13 – 8-15 there))

Endpoint filter (PLL) Parameters - 2

- However, many practical PLL implementations are based on a discrete time model where the integral block and VCO block of the PLL are modeled based on z-transforms
 - Depending on the details, this is mathematically equivalent to replacing derivatives by forward or backward differences
 - See Appendix I (Figure I-1 and Eq. (I-6)) of [8] and 3.5 of [9] for examples
 - As a result, the model becomes unstable if the sampling rate is not large enough compared to the PLL 3dB bandwidth
 - A common rule of thumb is that the sampling rate should be at least ten times the PLL bandwidth
 - The analysis in 3.5 of [9] shows that, for the example there, the theoretical limit for stability is approximately π times the 3dB bandwidth (i.e., the sampling rate must be at least π times the 3dB bandwidth for the PLL to be stable)
 - The PLL 3dB bandwidth above (used in simulations before those in [10]) of 2.5998 Hz implies that the sampling rate should be at least 25.998 Hz \cong 26 Hz based on the 10:1 rule of thumb
 - However, the sampling rate here is the Sync rate, and the minimum Sync rate corresponds to the maximum Sync interval, which is 131 ms
 - The minimum Sync rate is therefore $1/(0.131 \text{ s}) = 7.634 \text{ Hz}$, which is too small
 - The theoretical limit of $\pi:1$ implies a Sync rate of at least $(\pi)(2.6 \text{ Hz}) = 8.17 \text{ Hz}$, which still exceeds the 7.634 Hz minimum Sync rate

Endpoint filter (PLL) Parameters - 3

- ❑ To begin to address this, additional simulation cases were run in [10] with various PLL bandwidths smaller than 2.6 Hz (gain peaking was kept at 2.1985 dB)
 - The simulation cases of the current presentation consider PLL bandwidths in the range 0.5 Hz to 1.5 Hz
- ❑ However, as the PLL bandwidth becomes narrower, noise generation can become appreciable if the same oscillator is used, because the transfer function from the noise to the output is a high-pass filter with corner frequency and damping ratio the same as for the low-pass transfer function from the PLL input to output
- ❑ In the case here, it was indicated in one of the July 2023 60802 meetings that the same XO is used for the endpoint PLL filter as for the timestamping function

Endpoint filter (PLL) Parameters - 4

- Therefore, noise generation was modeled, using the same local oscillator phase variation model used for the LocalClock
 - The noise was computed by passing the XO phase noise through a high-pass filter with the same 3dB bandwidth and damping ratio as the low-pass PLL filter, and adding the result to the PLL output that was computed from the input
- It was intended that noise generation be modeled for the simulation cases of [13]; however, while the model was included in the simulator, the option to turn the noise generation on was accidentally not set
 - Noise generation was turned on for the corresponding simulation cases here; however, additional cases with noise generation turned off were also run so that the effect of the other updates to the assumptions could be seen (i.e., by comparing the results of [13] and the results here for the cases without noise generation)
- The gain peaking, and therefore the damping ratio, are kept at 2.1985 dB and 0.68219, respectively, for the simulation cases here

Simulation Cases - 1

- ❑ As indicated earlier, the drift tracking and compensation algorithms used here are described in detail in [1]
- ❑ In the notation below, $mNRR_{smoothingNA}$ is the number of Sync Intervals over which nRR is both computed and averaged, e.g., if $mNRR_{smoothingNA} = 4$, we compute nRR over 4 Sync intervals and average the 4 most recently computed values
- ❑ In the notation below, $mNRR_{compNAP}$ is the number of Sync Intervals over which the frequency drift rate estimate is computed
- ❑ All the simulation cases here use:
 - $mNRR_{compNAP} = 8$; $mNRR_{smoothingNA} = 4$
- ❑ The simulation cases are summarized on the following slide
 - The numbering of the simulation cases here follows the numbering in [10]
 - The simulation cases of [10] are numbered 1 through 28, with additional cases 5a, 6a, 7a, 8a, 25a, 26a, 27a, 28a
 - The simulation cases here with noise generation are numbered 29 through 35
 - The simulation cases here without noise generation are numbered 29a through 35a

Summary of Simulation Cases - 1

Case	Drift Tracking and Compensation (mNRRcompNAP, mNRRsmoothingNA)	PLL 3dB Bandwidth (Hz)	PLL noise generation present (yes/no)	GM noise magnitude relative to non-GM PTP Instances
29	(8, 4)	1.0	yes	0.5
30	(8, 4)	1.5	yes	0.5
31	(8, 4)	0.9	yes	0.5
32	(8, 4)	0.8	yes	0.5
33	(8, 4)	0.7	yes	0.5
34	(8, 4)	0.6	yes	0.5
35	(8, 4)	0.5	yes	0.5
29a	(8, 4)	1.0	no	0.5
30a	(8, 4)	1.5	no	0.5
31a	(8, 4)	0.9	no	0.5
32a	(8, 4)	0.8	no	0.5
33a	(8, 4)	0.7	no	0.5
34a	(8, 4)	0.6	no	0.5
35a	(8, 4)	0.5	no	0.5

Max $|dTE_R|$ Simulation Results for Cases with No Endpoint Filter Noise Generation

- ❑ Cases without endpoint filter noise generation are discussed first because these can be compared with results of [13] to see the effect of the changes in assumptions and corrections for items other than inclusion of noise generation
- ❑ Plots of max $|dTE_R|$ with no endpoint filter noise generation are presented on the following slides (27 – 36) for max $|dTE_R|$ before and after endpoint PLL filtering
- ❑ Filtered and unfiltered max $|dTE_R|$ for nodes 65 and 101 with no endpoint filter noise generation are summarized in the table on slide 37; results from [13] are also shown, for comparison
- ❑ Slide 27 shows 99% confidence intervals for the 0.95 quantile and maximum over 300 replications, for cases 29a – 35a
- ❑ Slide 28 shows maximum over 300 replications, for cases 29a– 35a
- ❑ Slide 29 shows unfiltered max $|dTE_R|$ (it is the same for all six cases because only the filter bandwidth varies for these cases)
 - The remaining plots show the 99% confidence intervals for the 0.95 quantile and maximum over 300 replications for each case individually; these plots are provided because the plots showing all the cases together are fairly cluttered

Filtered max $|dTE_R|$, Cases 29a - 35a

Cases 29a, 30a, 31a, 32a, 33a, 34a, 35a - mult replic results - filt
GM time error modeled; dTE_R is relative to GM

GM labeled node 1

Algorithms of Annex D

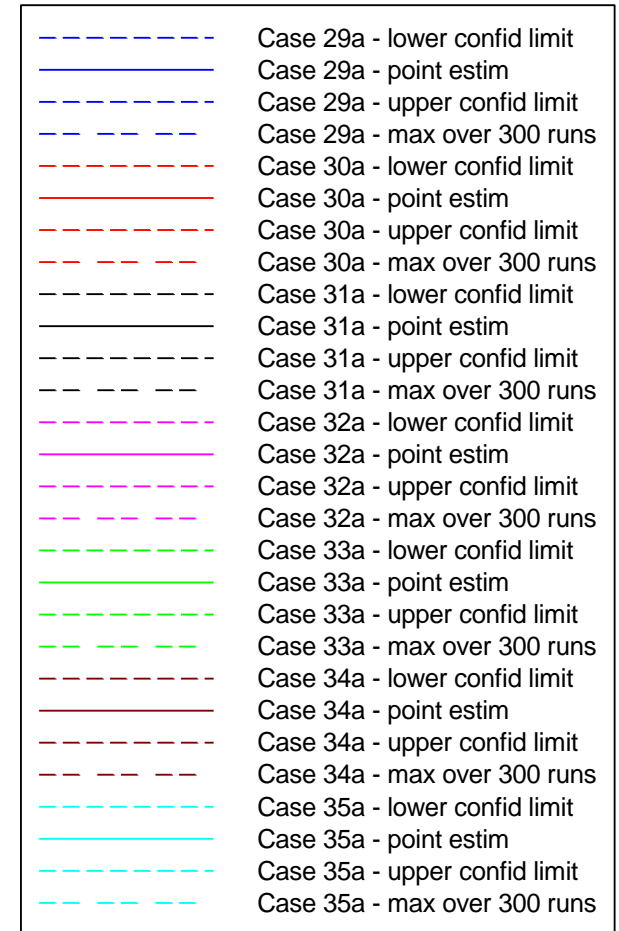
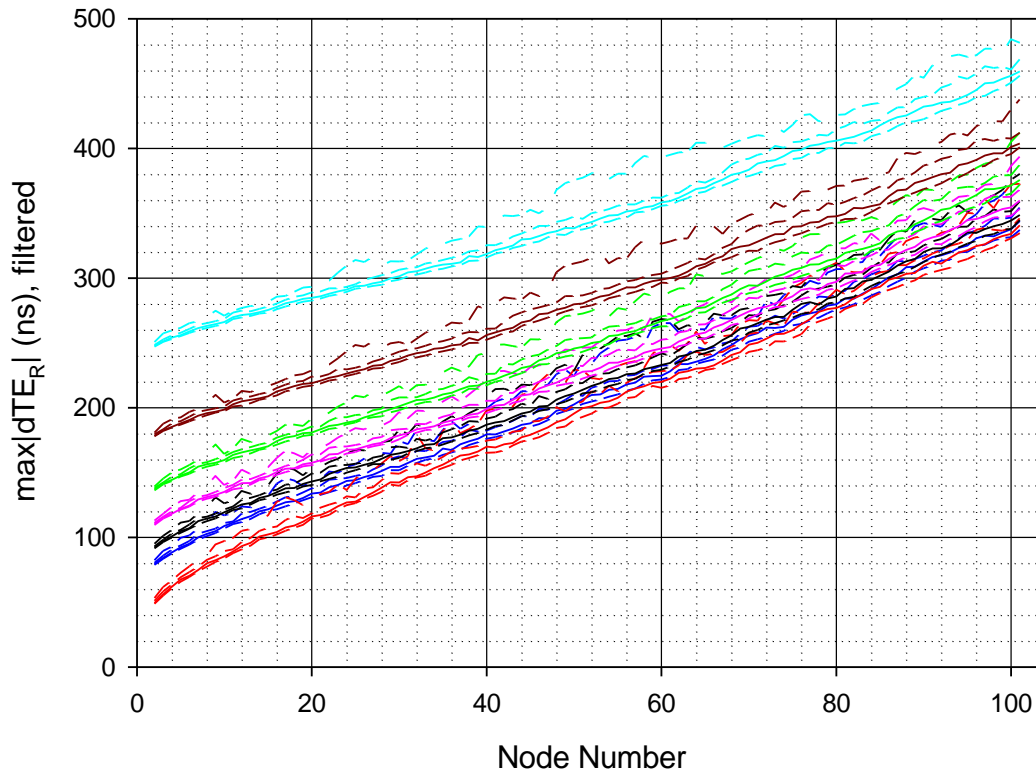
Gain peaking = 0.1 dB

3dB BWs for cases 29-33: 1.0, 1.5, 0.9, 0.8, 0.7, 0.6, 0.5 Hz

No endpoint filter noise generation

Temp profile: half-sinusoid with 95 s period and 30 s dwell, -40 to +85 C

XO freq stability



Filtered max $|dTE_R|$, Cases 29a - 35a, max over 300 runs

Cases 29a, 30a, 31a, 32a, 33a, 34a, 35a - mult replic results - filt
GM time error modeled; dTE_R is relative to GM

GM labeled node 1

Algorithms of Annex D

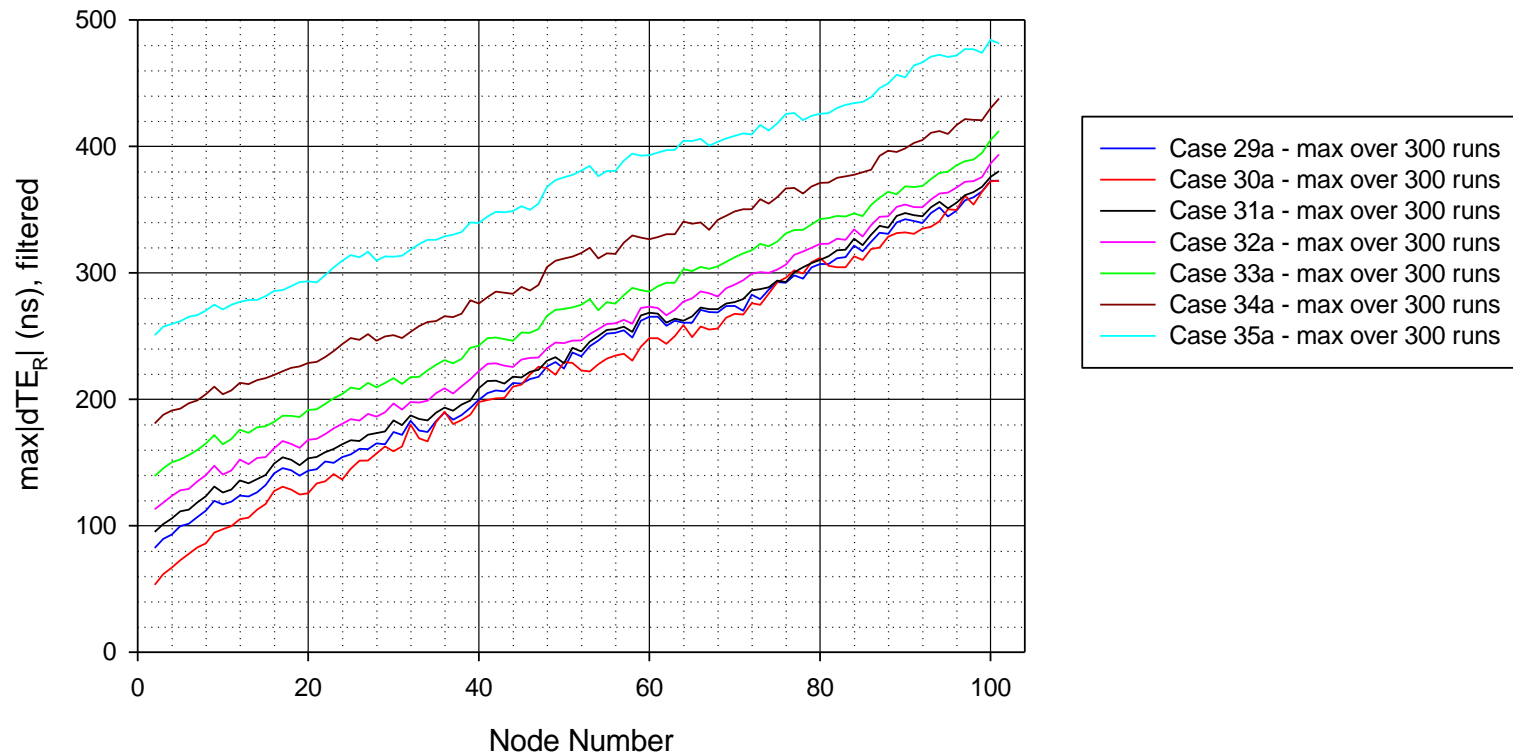
Gain peaking = 0.1 dB

3dB BWs for cases 29-33: 1.0, 1.5, 0.9, 0.8, 0.7, 0.6, 0.5 Hz

No endpoint filter noise generation

Temp profile: half-sinusoid with 95 s period and 30 s dwell, -40 to +85 C

XO freq stability



Unfiltered max $|dTE_R|$, Cases 29 - 35 (same for all cases)

Cases 29, 30, 31, 32, 33 - mult replic results - unfilt

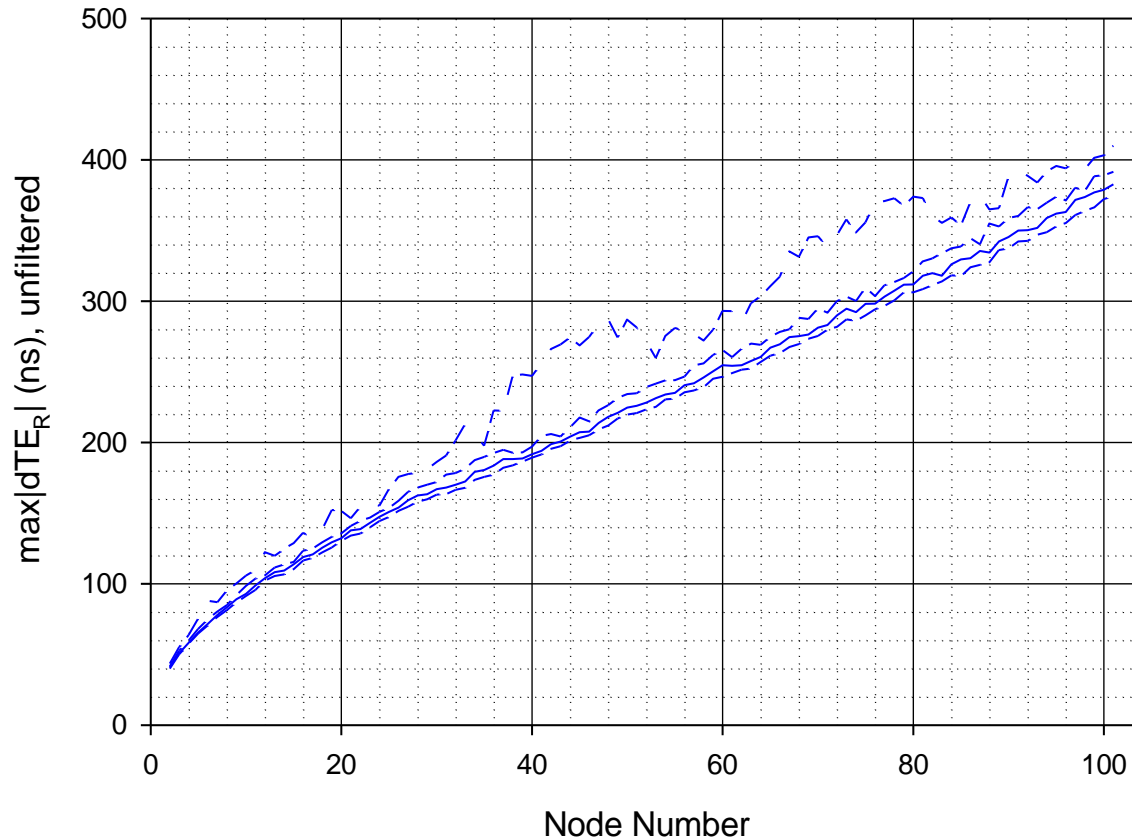
Results are the same for all the cases since they differ only in filt BW

GM time error modeled; dTE_R is relative to GM; GM labeled node 1

Algorithms of Annex D

Temp profile: half-sinusoid with 95 s period and 30 s dwell, -40 to +85 C

XO freq stability



Filtered max $|dTE_R|$, Case 29a

Case 29 - mult replic results - filt

GM time error modeled; dTE_R is relative to GM

GM labeled node 1

Algorithms of Annex D

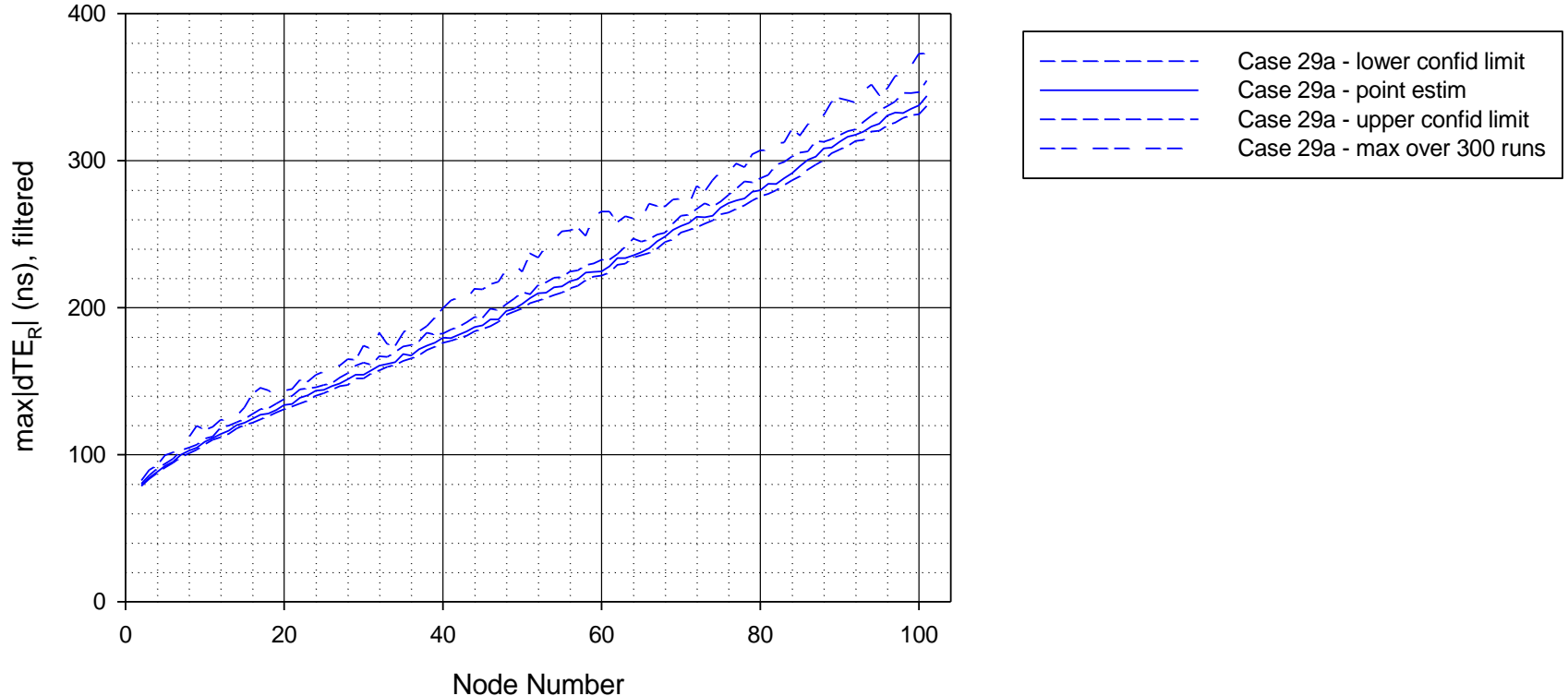
Gain peaking = 0.1 dB

3dB BW: 1.0 Hz

No endpoint filter noise generation

Temp profile: half-sinusoid with 95 s period and 30 s dwell, -40 to +85 C

XO freq stability



Filtered max $|dTE_R|$, Case 30a

Case 30a - mult replic results - filt

GM time error modeled; dTE_R is relative to GM

GM labeled node 1

Algorithms of Annex D

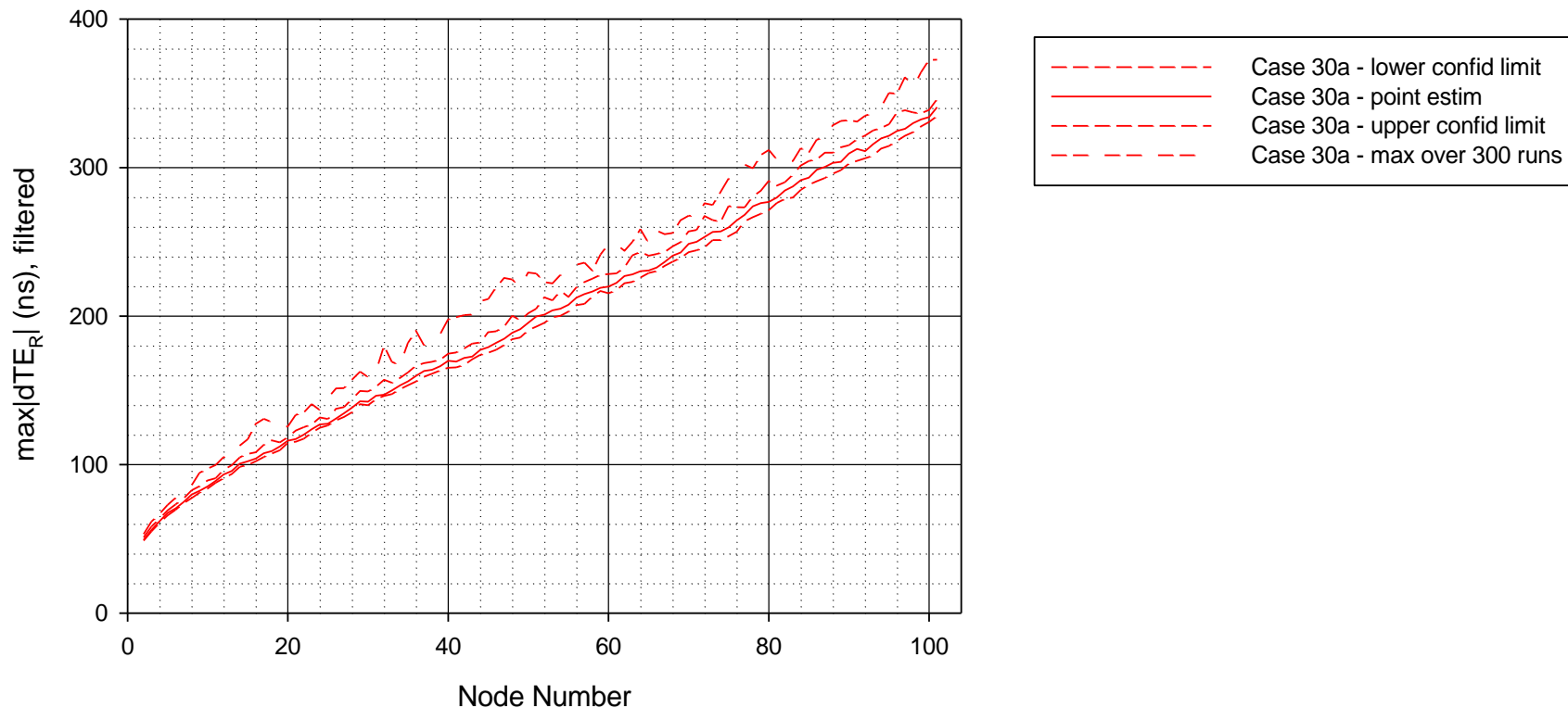
Gain peaking = 0.1 dB

3dB BW: 1.5 Hz

No endpoint filter noise generation

Temp profile: half-sinusoid with 95 s period and 30 s dwell, -40 to +85 C

XO freq stability



Filtered max $|dTE_R|$, Case 31a

Case 31a - mult replic results - filt

GM time error modeled; dTE_R is relative to GM

GM labeled node 1

Algorithms of Annex D

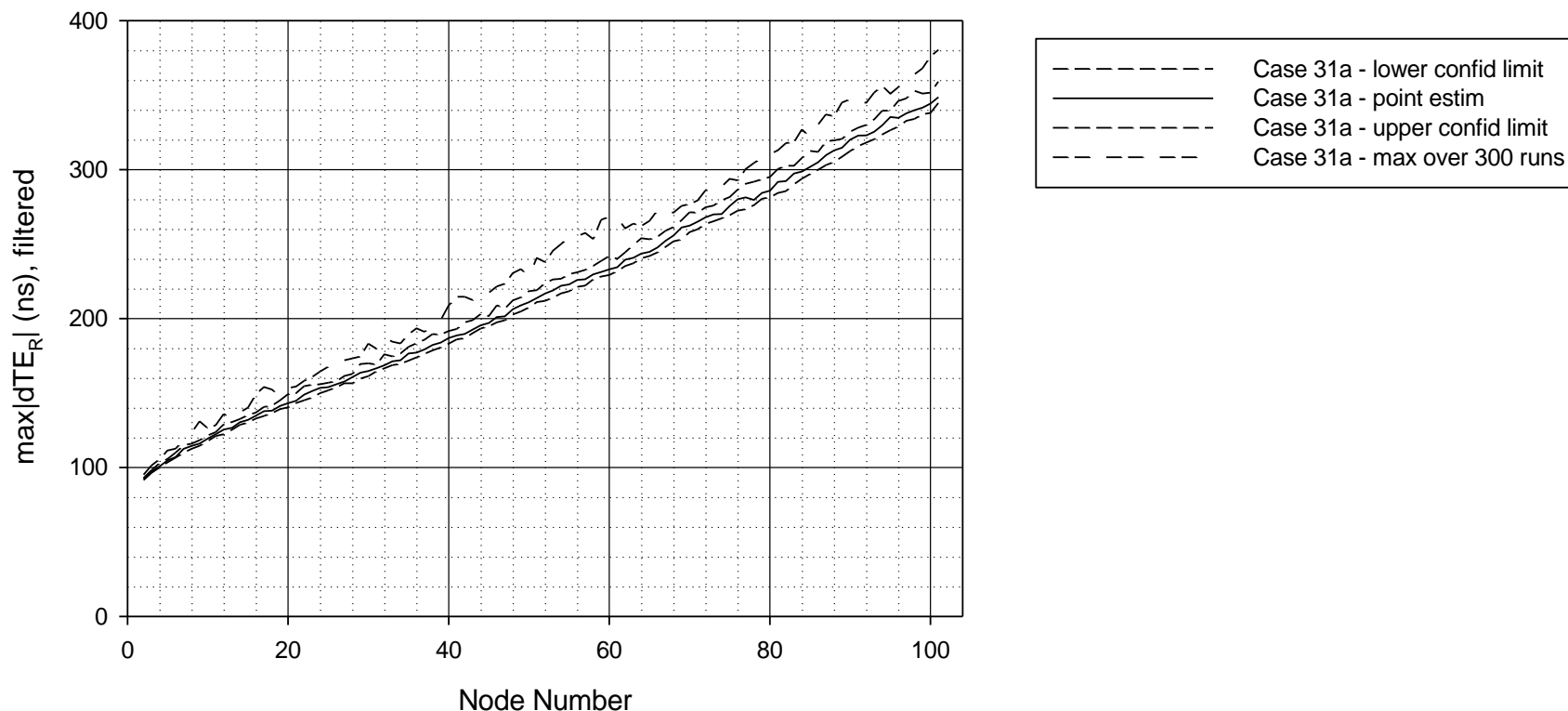
Gain peaking = 0.1 dB

3dB BW: 0.9 Hz

No endpoint filter noise generation

Temp profile: half-sinusoid with 95 s period and 30 s dwell, -40 to +85 C

XO freq stability



Filtered max $|dTE_R|$, Case 32a

Case 32a - mult replic results - filt

GM time error modeled; dTE_R is relative to GM

GM labeled node 1

Algorithms of Annex D

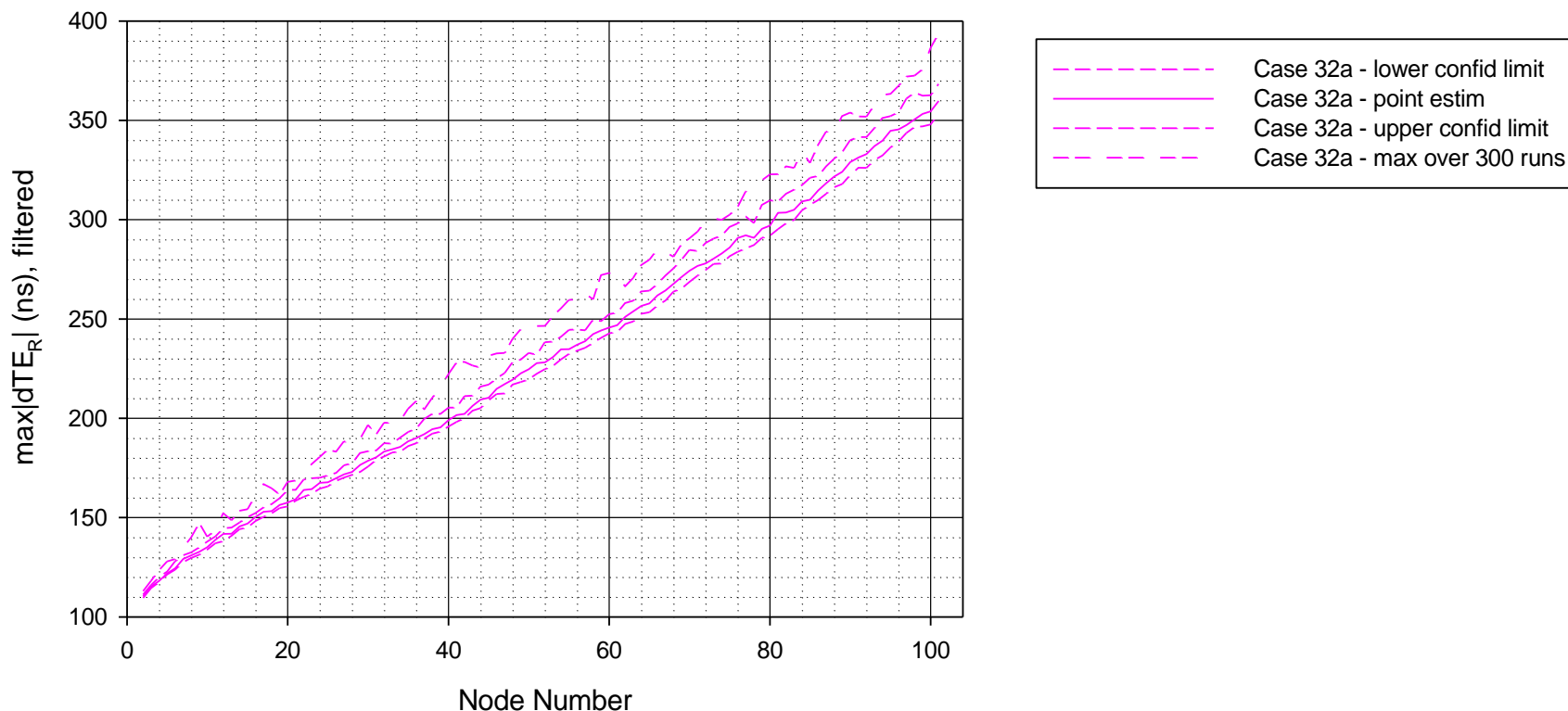
Gain peaking = 0.1 dB

3dB BW: 0.8 Hz

No endpoint filter noise generation

Temp profile: half-sinusoid with 95 s period and 30 s dwell, -40 to +85 C

XO freq stability



Filtered max $|dTE_R|$, Case 33a

Case 33a - mult replic results - filt

GM time error modeled; dTE_R is relative to GM

GM labeled node 1

Algorithms of Annex D

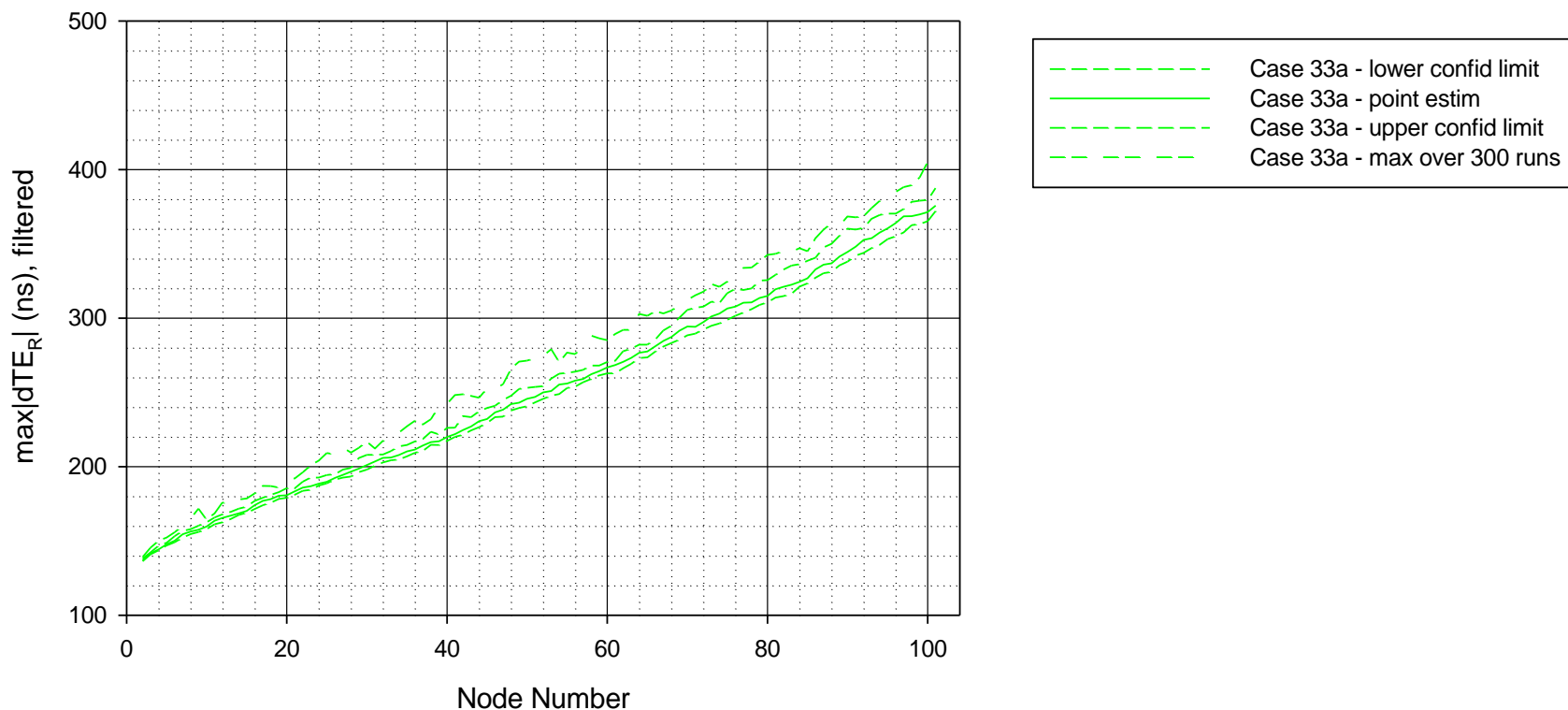
Gain peaking = 0.1 dB

3dB BW: 0.7 Hz

No endpoint filter noise generation

Temp profile: half-sinusoid with 95 s period and 30 s dwell, -40 to +85 C

XO freq stability



Filtered max $|dTE_R|$, Case 34a

Case 34a - mult replic results - filt

GM time error modeled; dTE_R is relative to GM

GM labeled node 1

Algorithms of Annex D

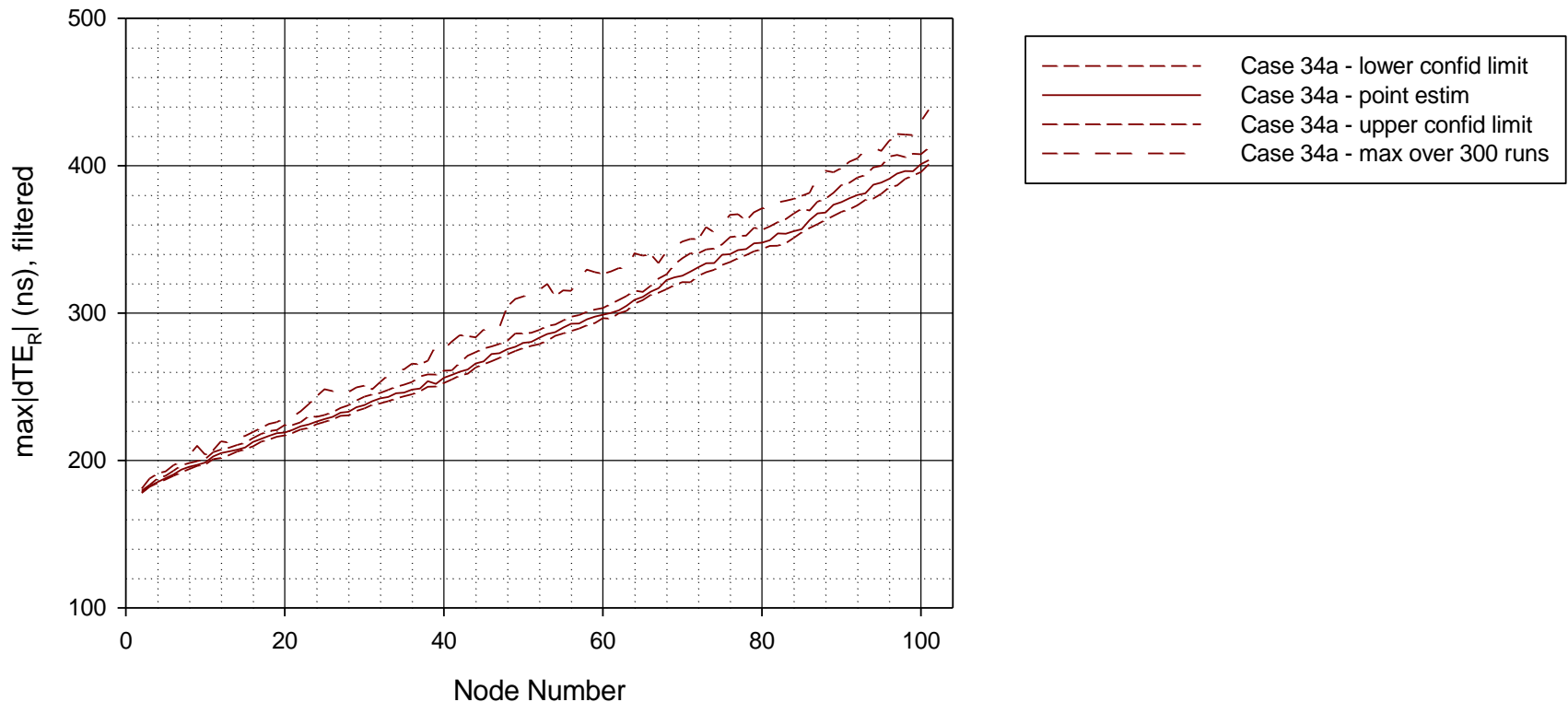
Gain peaking = 0.1 dB

3dB BW: 0.6 Hz

No endpoint filter noise generation

Temp profile: half-sinusoid with 95 s period and 30 s dwell, -40 to +85 C

XO freq stability



Filtered max $|dTE_R|$, Case 35a

Case 35a - mult replic results - filt

GM time error modeled; dTE_R is relative to GM

GM labeled node 1

Algorithms of Annex D

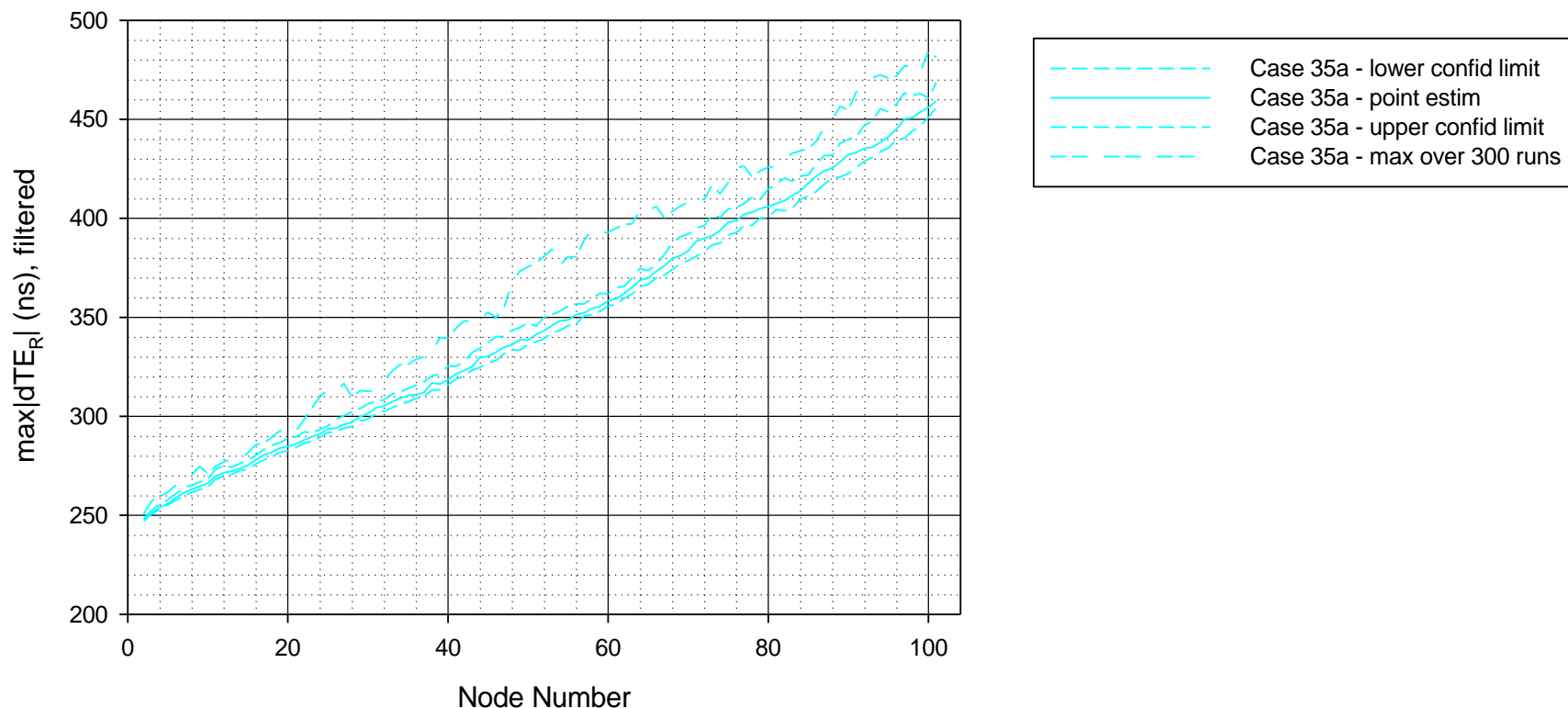
Gain peaking = 0.1 dB

3dB BW: 0.5 Hz

No endpoint filter noise generation

Temp profile: half-sinusoid with 95 s period and 30 s dwell, -40 to +85 C

XO freq stability



Summary of Filtered $\max|dTE_R|$ Results at Nodes 65 and 101 for Cases without Noise Generation

Case	PLL 3dB Bandwidth (Hz)	Filtered $\max dTE_R $ Node 65 (ns)	Filtered $\max dTE_R $ Node 65 Results from [13] (ns)	Filtered $\max dTE_R $ Node 101 (ns)	Filtered $\max dTE_R $ Node 101 Results from [13] (ns)
30a	1.5	249.1	339.4	372.7	507.8
29a	1.0	260.4	337.4	372.9	498.7
31a	0.9	265.6	347.3	380.4	497.6
32a	0.8	279.8	358.7	393.7	497.2
33a	0.7	301.4	372.4	412.1	498.4
34a	0.6	338.8	394.1	437.8	504.6
35a	0.5	404.1	441.5	481.3	535.7
unfiltered	-	310.5	363.5	410.0	548.9

Note 1: Unfiltered results are the same for all cases (29 – 35 and 29a – 35a) because the cases differ only in the filter bandwidth

Note 2: Case 29 follows case 30 so that cases are in order of decreasing endpoint filter bandwidth

Discussion of $\max|dTE_R|$ Results for Cases without Endpoint Filter Noise Generation - 1

- For cases without endpoint filter noise generation, the 500 ns objective for $\max|dTE_R|$ is met after 100 hops (i.e., at node 101) for all cases, i.e., for endpoint filter bandwidths in the range 0.5 Hz to 1.5 Hz
 - The results indicate that the objective would be met over an even wider range
- The results are less than the results of [13]; it is likely that the most significant effect is the new assumption that the random variation in Sync interval, Pdelay interval, residence time, and pdelay turnaround time is relative to the ideal simulator clock rather than the local clock
 - As indicated earlier, the effect of TSGE caused the jumps on the order of 4 ns that were seen in computed unfiltered mean path delay in [15]; with this revised assumption, the jumps were subsequently eliminated in [14]
- Unlike the results of [13], the new results increase uniformly as bandwidth is decreased
 - It appears that any added filtering due to a smaller bandwidth, which would tend to filter incoming phase/time variation and decrease $\max|dTE_R|$, is more than offset by the longer time over which incoming information from upstream is incorporated into the time estimate

Discussion of $\max|dTE_R|$ Results for Cases without Endpoint Filter Noise Generation - 2

- For the cases here, $\max|dTE_R|$ increases from 372.7 ns for a bandwidth of 1.5 Hz to 481.3 ns for a bandwidth of 0.5 Hz
 - $\max|dTE_R|$ is 410.0 ns for no endpoint filtering
 - Note that the case of no endpoint filtering actually corresponds to filtering at the Nyquist frequency
 - The Nyquist frequency one-half the sampling rate, which can be taken as one-half the minimum Sync rate, i.e., $(0.5)(1/0.131 \text{ s}) = (0.5)(7.634 \text{ Hz}) = 3.817 \text{ Hz}$
 - The Nyquist frequency is larger than the largest endpoint filter bandwidth simulated here, i.e., 1.5 Hz, which is consistent with $\max|dTE_R|$ for the case of no endpoint filtering being smaller than for the case of 1.5 Hz endpoint filter bandwidth
 - It is possible that, with further increase in bandwidth from 1.5 Hz to the Nyquist frequency, $\max|dTE_R|$ would increase

Max $|dTE_R|$ Simulation Results for Cases with Endpoint Filter Noise Generation

- ❑ Cases with endpoint filter noise generation are of most interest
- ❑ Plots of $\max|dTE_R|$ with no endpoint filter noise generation are presented on the following slides (41 – 50) for $\max|dTE_R|$ before and after endpoint PLL filtering
- ❑ Filtered and unfiltered $\max|dTE_R|$ for nodes 65 and 101 with no endpoint filter noise generation are summarized in the table on slide 51
- ❑ Slide 41 shows 99% confidence intervals for the 0.95 quantile and maximum over 300 replications, for cases 29 – 35
- ❑ Slide 42 shows maximum over 300 replications, for cases 29– 35
- ❑ Slide 43 shows unfiltered $\max|dTE_R|$ (it is the same for all six cases because only the filter bandwidth varies for these cases)
 - The remaining plots show the 99% confidence intervals for the 0.95 quantile and maximum over 300 replications for each case individually; these plots are provided because the plots showing all the cases together are fairly cluttered

Filtered max |dTE_R|, Cases 29 - 35

Cases 29, 30, 31, 32, 33, 34, 35 - mult replic results - filt
GM time error modeled; dTE_R is relative to GM

GM labeled node 1

Algorithms of Annex D

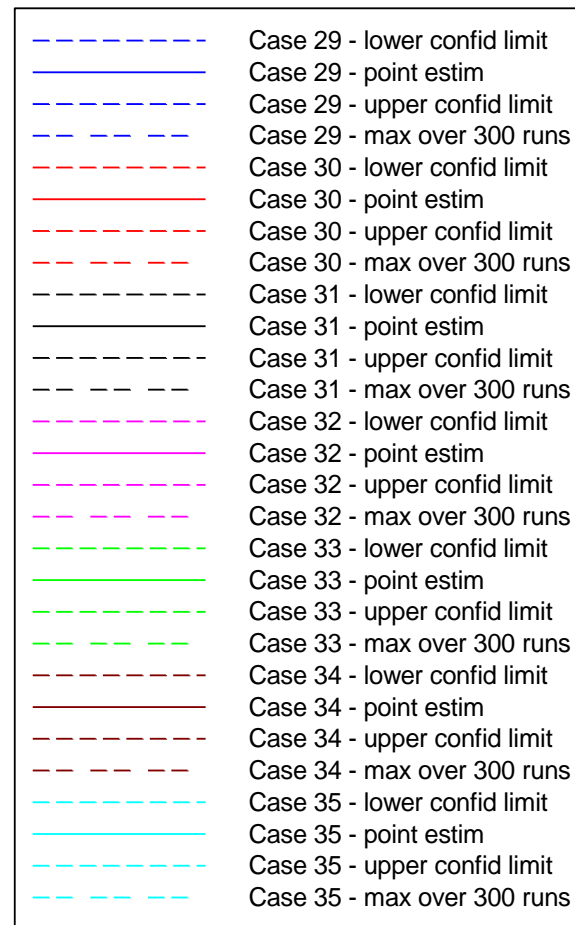
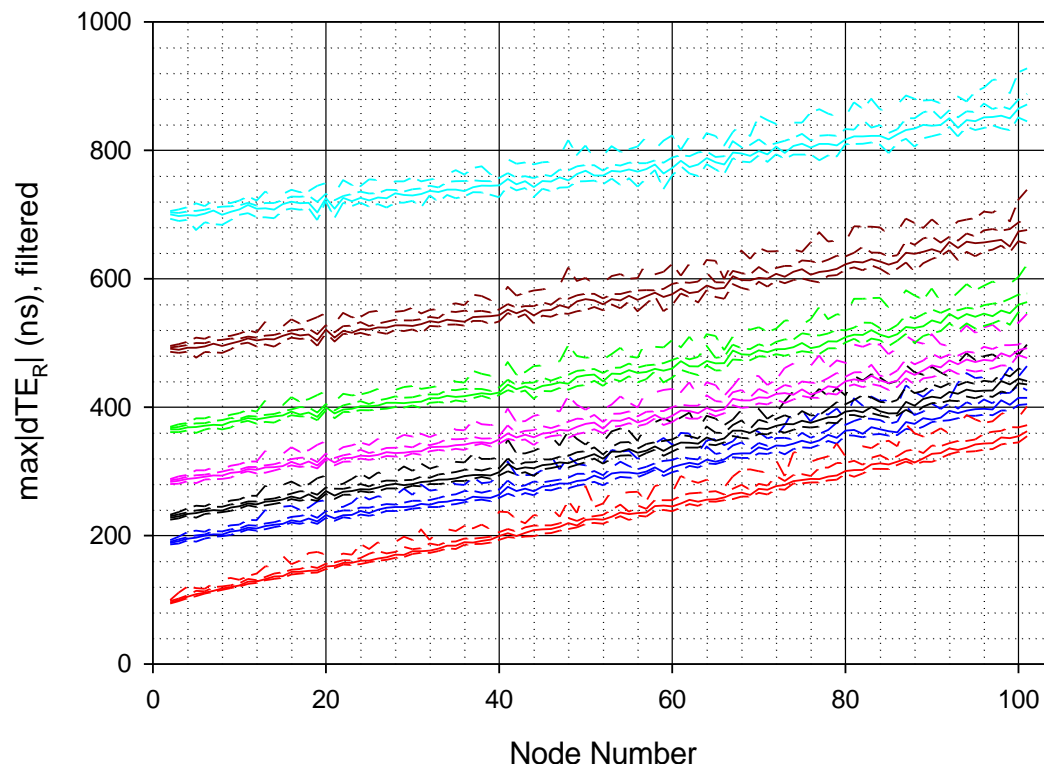
Gain peaking = 0.1 dB

3dB BWs for cases 29-33: 1.0, 1.5, 0.9, 0.8, 0.7, 0.6, 0.5 Hz

Endpoint filter noise generation modeled

Temp profile: half-sinusoid with 95 s period and 30 s dwell, -40 to +85 C

XO freq stability



Filtered max $|dTE_R|$, Cases 29 - 35, max over 300 runs

Cases 29, 30, 31, 32, 33, 34, 35 - mult replic results - filt
GM time error modeled; dTE_R is relative to GM

GM labeled node 1

Algorithms of Annex D

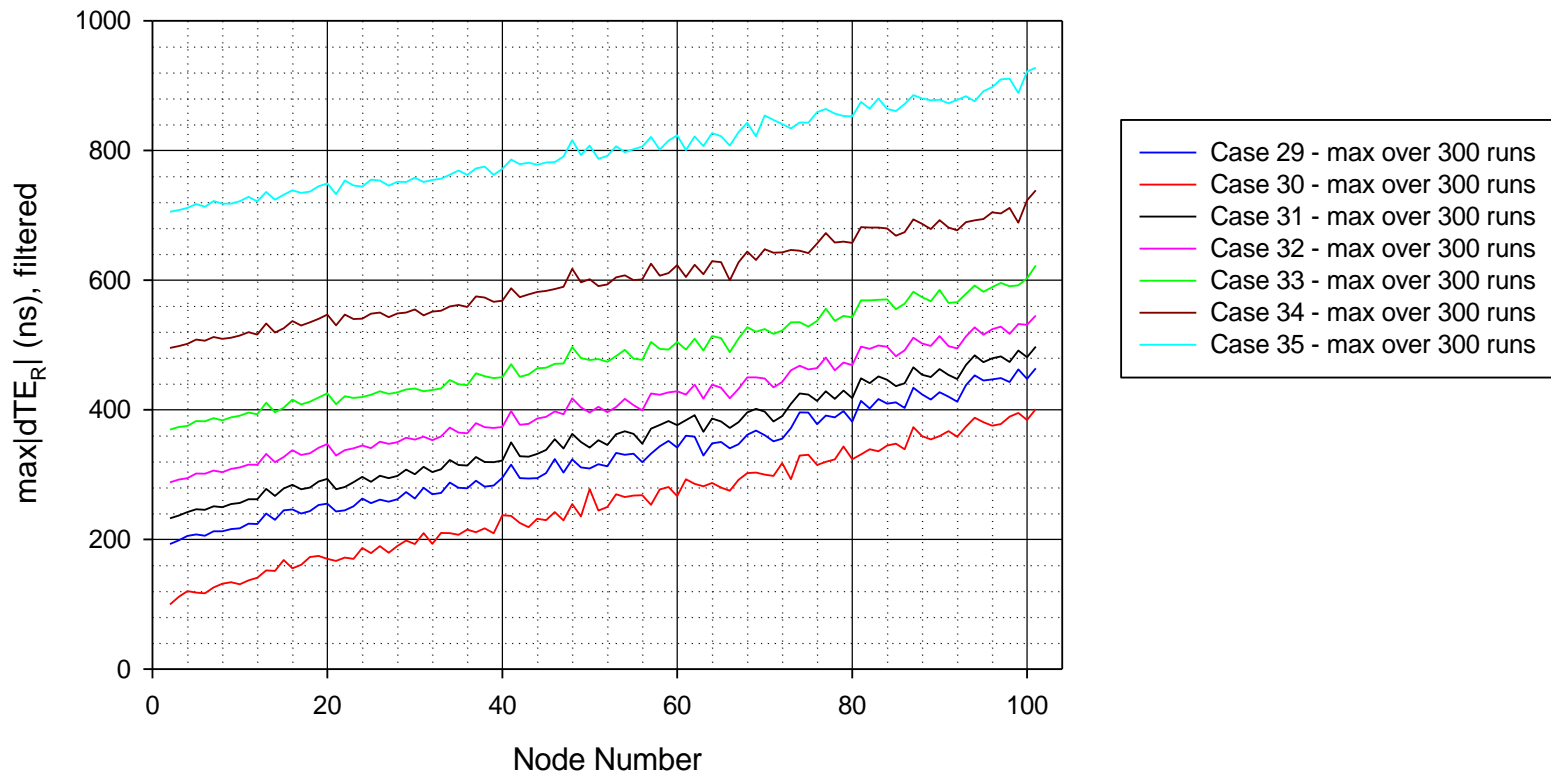
Gain peaking = 0.1 dB

3dB BWs for cases 29-33: 1.0, 1.5, 0.9, 0.8, 0.7, 0.6, 0.5 Hz

Endpoint filter noise generation modeled

Temp profile: half-sinusoid with 95 s period and 30 s dwell, -40 to +85 C

XO freq stability



Unfiltered max $|dTE_R|$, Cases 29 - 35 (same for all cases)

Cases 29, 30, 31, 32, 33 - mult replic results - unfilt

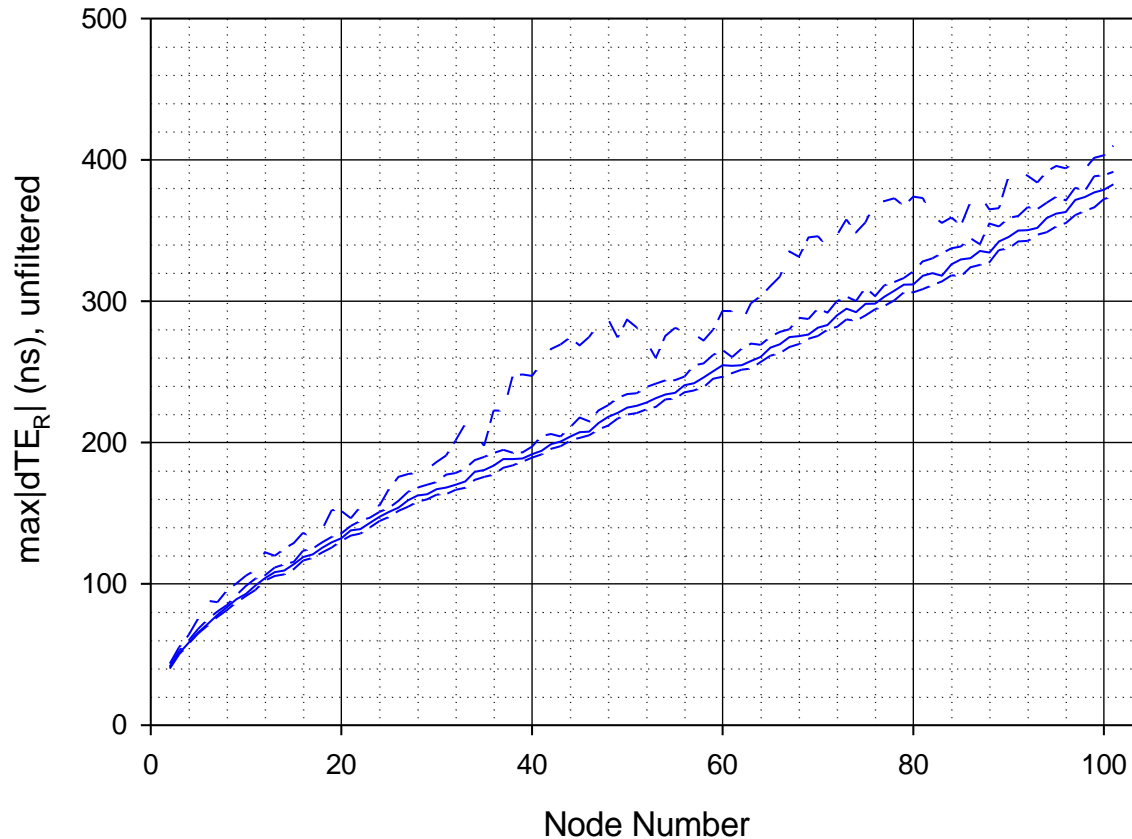
Results are the same for all the cases since they differ only in filt BW

GM time error modeled; dTE_R is relative to GM; GM labeled node 1

Algorithms of Annex D

Temp profile: half-sinusoid with 95 s period and 30 s dwell, -40 to +85 C

XO freq stability



Filtered max $|dTE_R|$, Case 29

Case 29 - mult replic results - filt

GM time error modeled; dTE_R is relative to GM

GM labeled node 1

Algorithms of Annex D

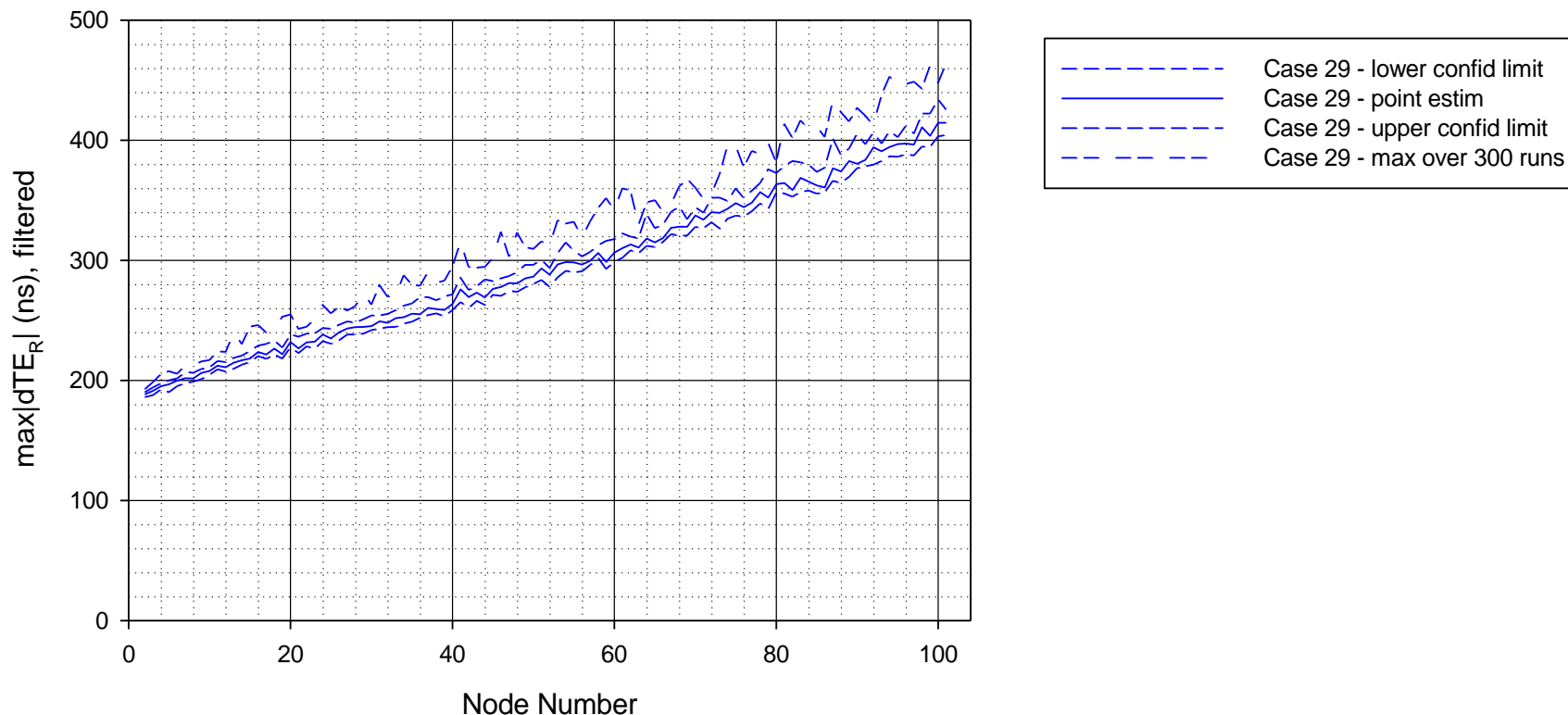
Gain peaking = 0.1 dB

3dB BW: 1.0 Hz

Endpoint filter noise generation modeled

Temp profile: half-sinusoid with 95 s period and 30 s dwell, -40 to +85 C

XO freq stability



Filtered max $|dTE_R|$, Case 30

Case 30 - mult replic results - filt

GM time error modeled; dTE_R is relative to GM

GM labeled node 1

Algorithms of Annex D

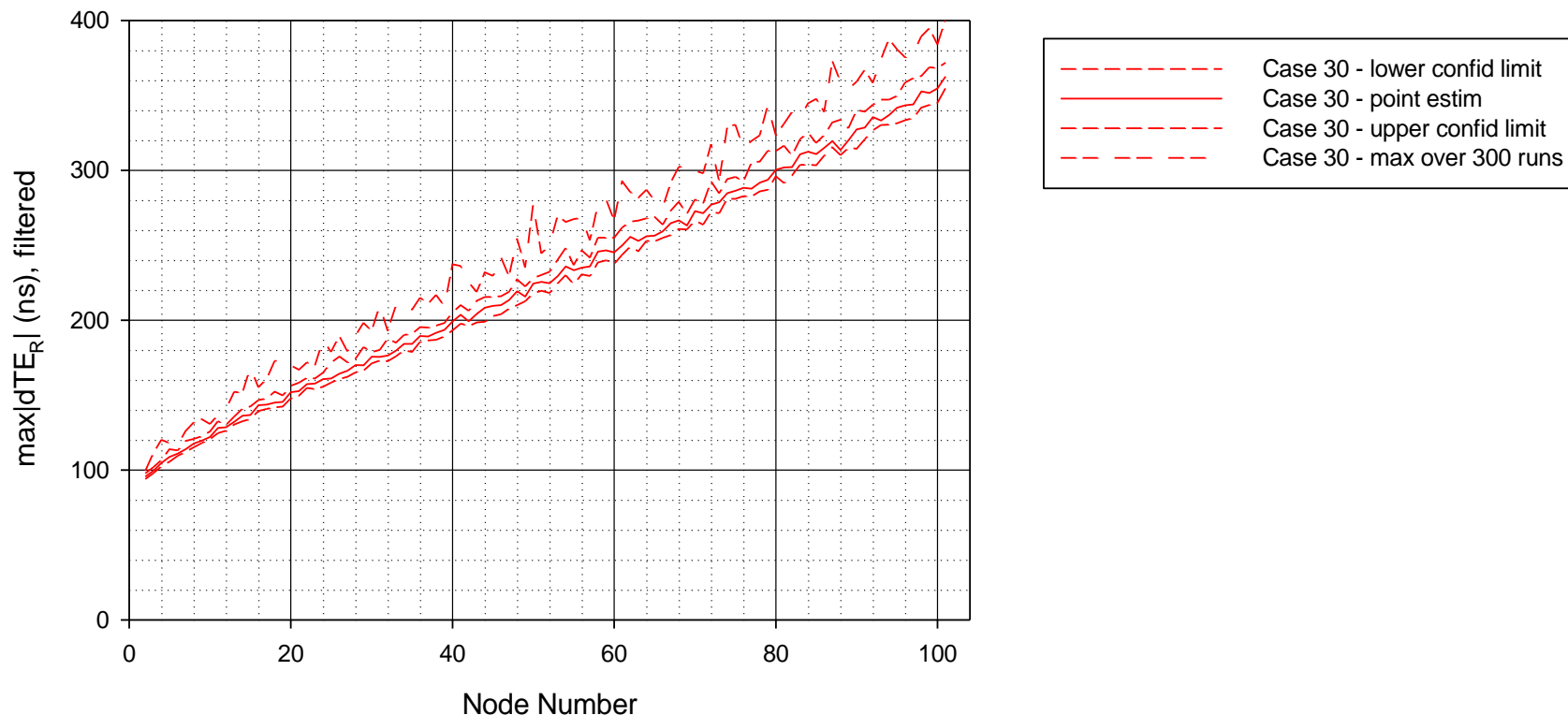
Gain peaking = 0.1 dB

3dB BW: 1.5 Hz

Endpoint filter noise generation modeled

Temp profile: half-sinusoid with 95 s period and 30 s dwell, -40 to +85 C

XO freq stability



Filtered max $|dTE_R|$, Case 31

Case 31 - mult replic results - filt

GM time error modeled; dTE_R is relative to GM

GM labeled node 1

Algorithms of Annex D

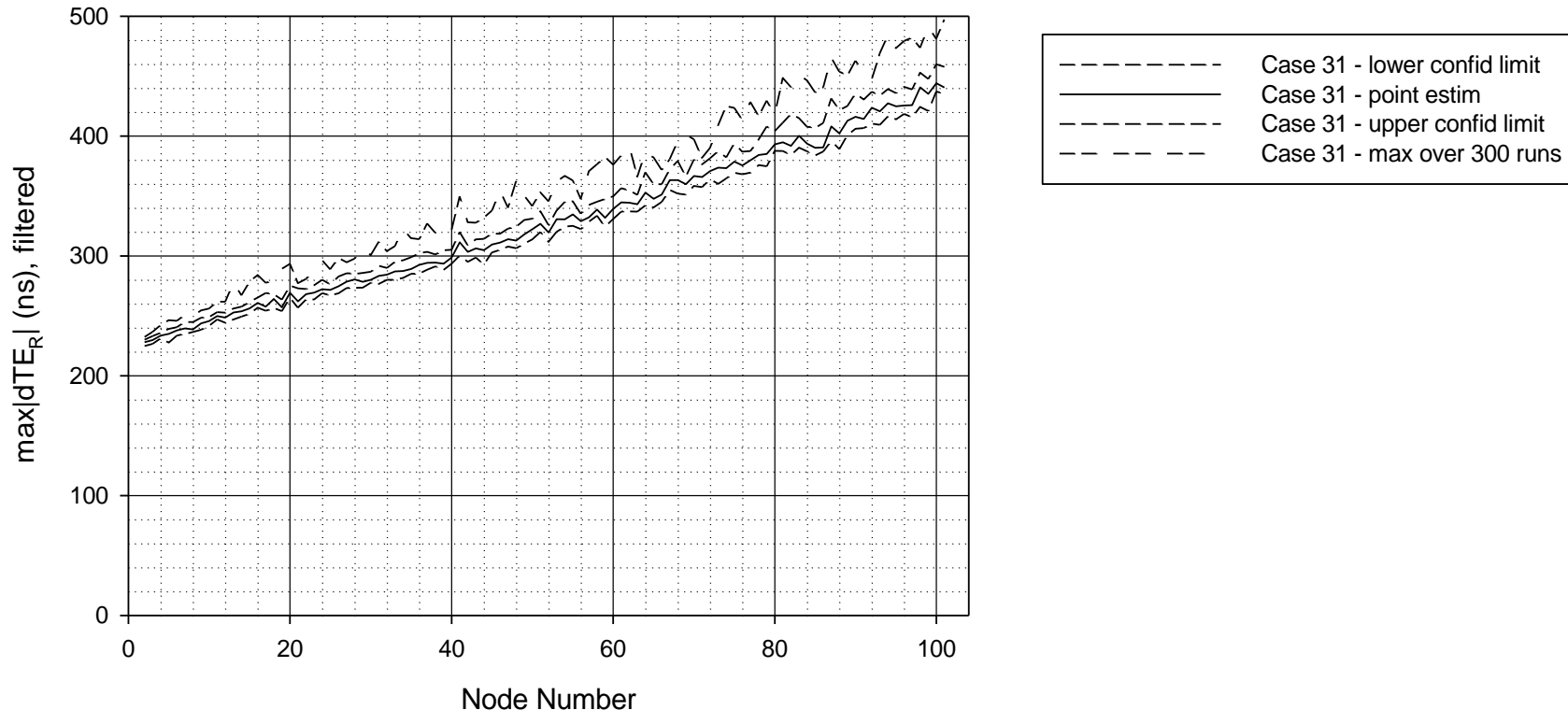
Gain peaking = 0.1 dB

3dB BW: 0.9 Hz

Endpoint filter noise generation modeled

Temp profile: half-sinusoid with 95 s period and 30 s dwell, -40 to +85 C

XO freq stability



Filtered max $|dTE_R|$, Case 32

Case 32 - mult replic results - filt

GM time error modeled; dTE_R is relative to GM

GM labeled node 1

Algorithms of Annex D

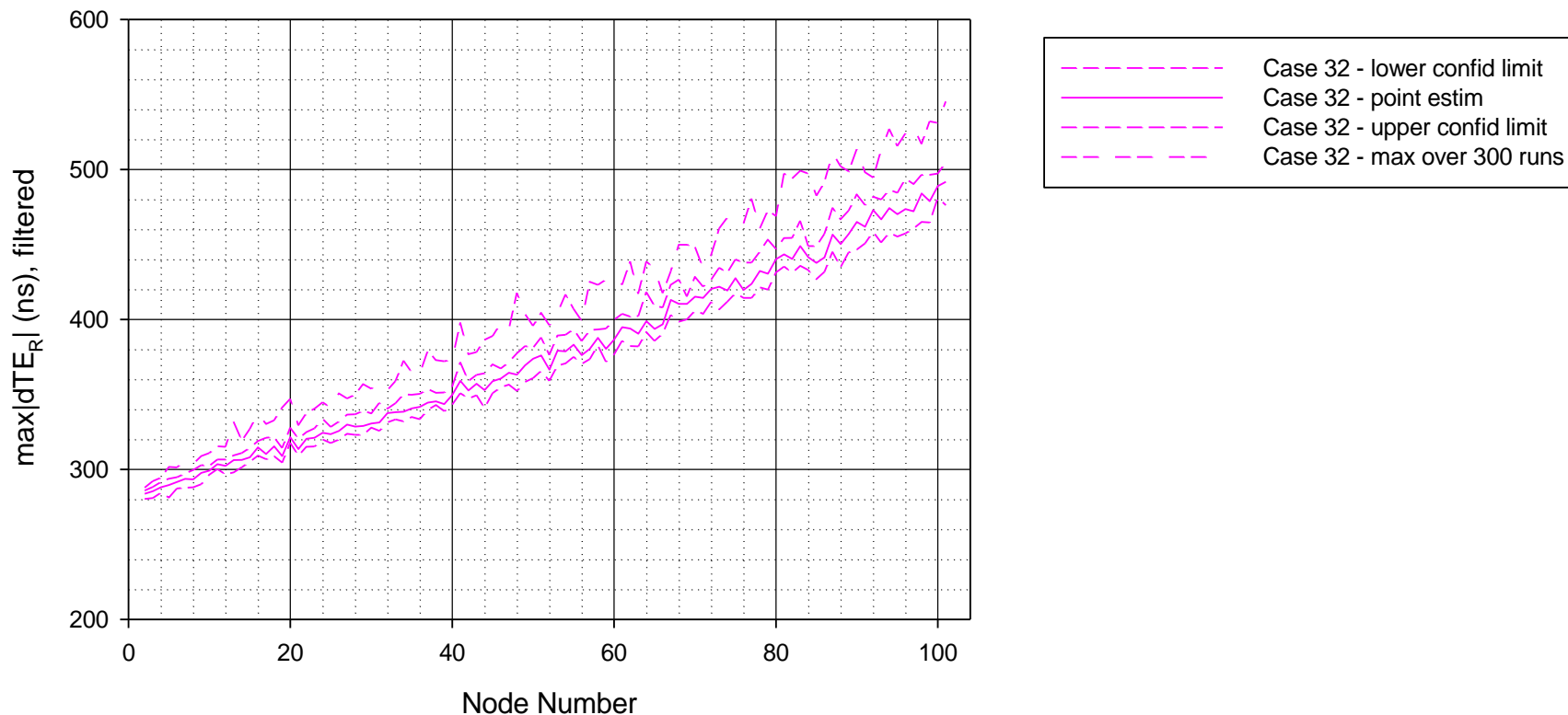
Gain peaking = 0.1 dB

3dB BW: 0.8 Hz

Endpoint filter noise generation modeled

Temp profile: half-sinusoid with 95 s period and 30 s dwell, -40 to +85 C

XO freq stability



Filtered max $|dTE_R|$, Case 33

Case 33 - mult replic results - filt

GM time error modeled; dTE_R is relative to GM

GM labeled node 1

Algorithms of Annex D

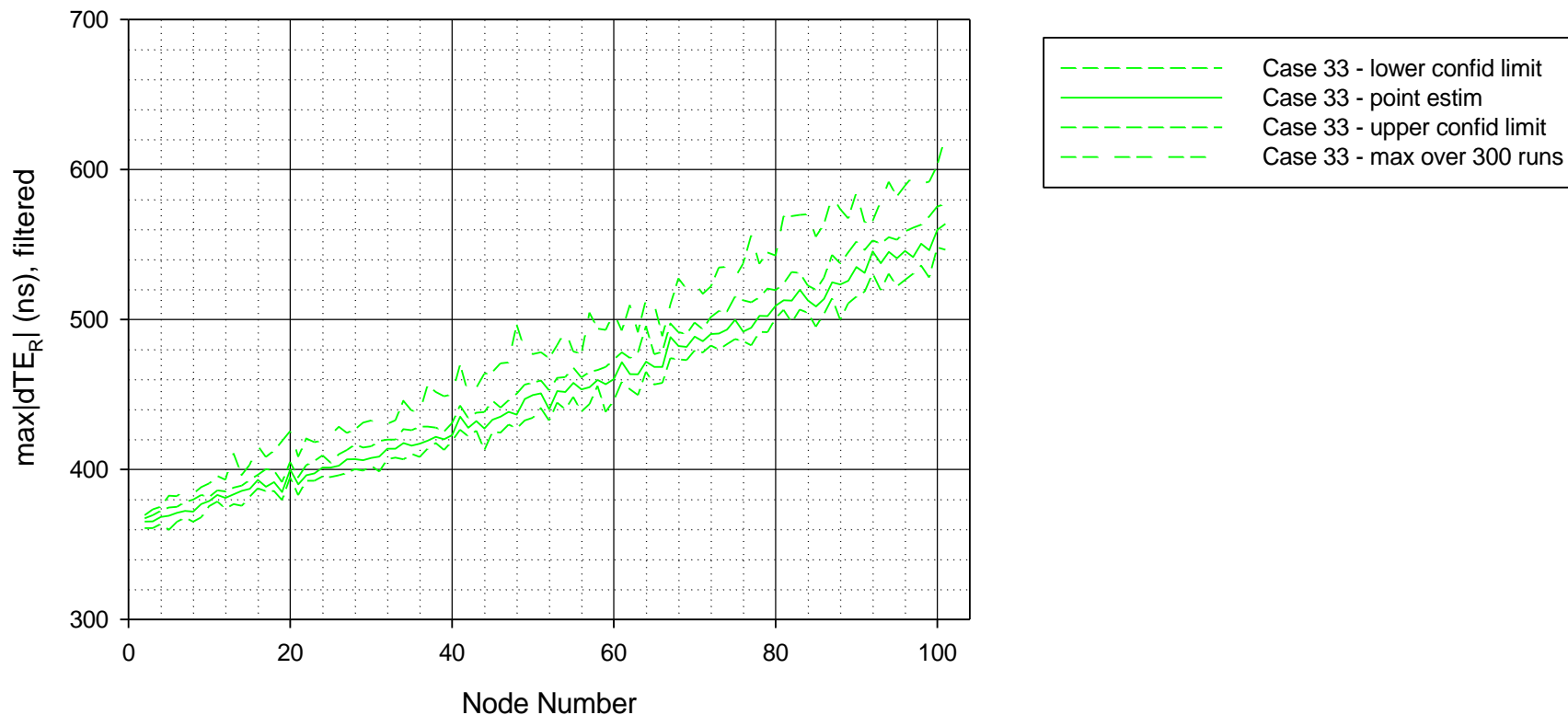
Gain peaking = 0.1 dB

3dB BW: 0.7 Hz

Endpoint filter noise generation modeled

Temp profile: half-sinusoid with 95 s period and 30 s dwell, -40 to +85 C

XO freq stability



Filtered max $|dTE_R|$, Case 34

Case 34 - mult replic results - filt

GM time error modeled; dTE_R is relative to GM

GM labeled node 1

Algorithms of Annex D

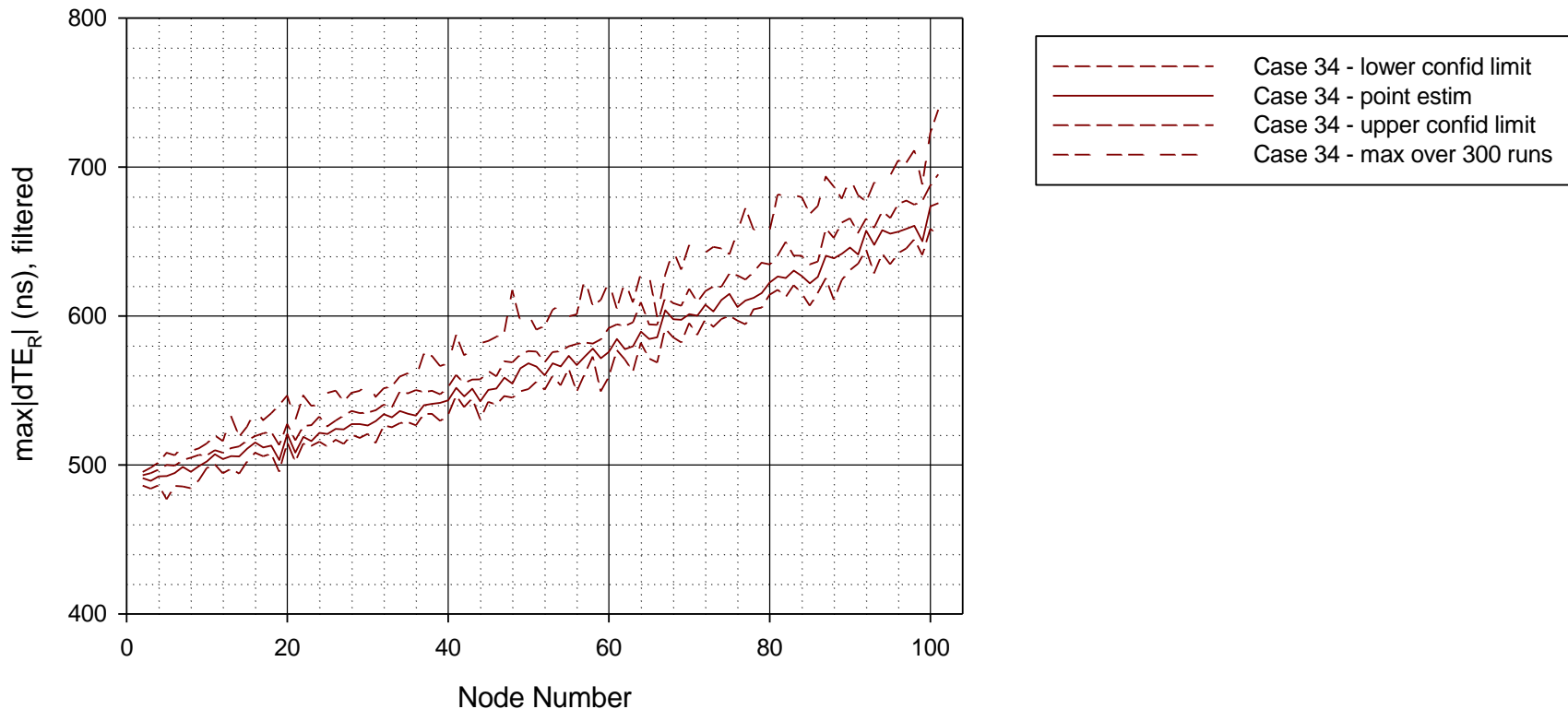
Gain peaking = 0.1 dB

3dB BW: 0.6 Hz

Endpoint filter noise generation modeled

Temp profile: half-sinusoid with 95 s period and 30 s dwell, -40 to +85 C

XO freq stability



Filtered max $|dTE_R|$, Case 35

Case 35 - mult replic results - filt

GM time error modeled; dTE_R is relative to GM

GM labeled node 1

Algorithms of Annex D

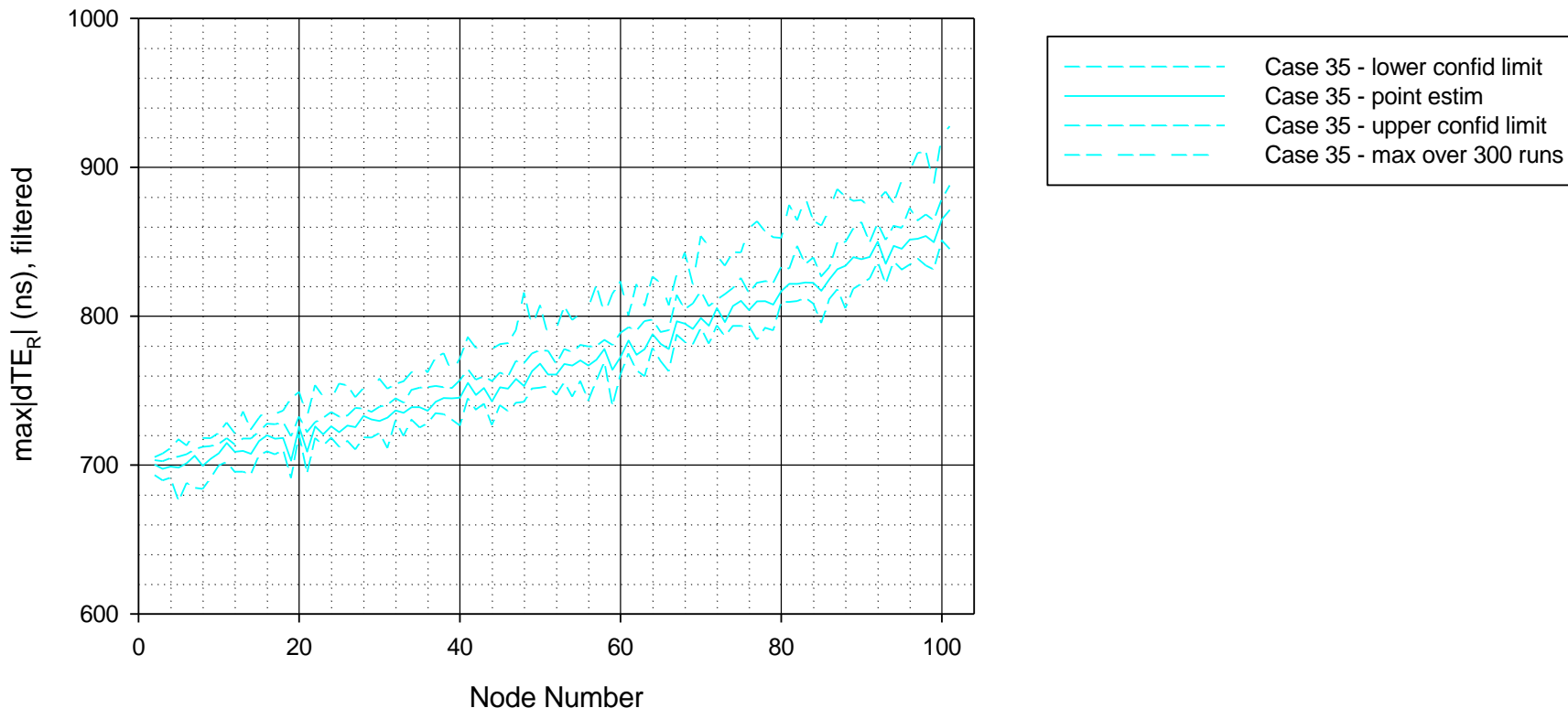
Gain peaking = 0.1 dB

3dB BW: 0.5 Hz

Endpoint filter noise generation modeled

Temp profile: half-sinusoid with 95 s period and 30 s dwell, -40 to +85 C

XO freq stability



Summary of Filtered $\max|dTE_R|$ Results at Nodes 65 and 101 for Cases with Noise Generation

Case	PLL 3dB Bandwidth (Hz)	Filtered $\max dTE_R $ Node 65 (ns)	Filtered $\max dTE_R $ Node 101 (ns)
30	1.5	279.8	400.9
29	1.0	350.0	463.9
31	0.9	381.9	497.2
32	0.8	433.8	545.3
33	0.7	510.5	622.3
34	0.6	627.5	738.4
35	0.5	821.9	927.5
unfiltered	-	310.5	410.0

Note 1: Unfiltered results are the same for all cases (29 – 35 and 29a – 35a) because the cases differ only in the filter bandwidth

Note 2: Case 29 follows case 30 so that cases are in order of decreasing endpoint filter bandwidth

Discussion of $\max|dTE_R|$ Results for Cases with Endpoint Filter Noise Generation - 1

- For cases with endpoint filter noise generation, the 500 ns objective for $\max|dTE_R|$ is met after 100 hops (i.e., at node 101) for cases 29, 30, and 31, i.e., for endpoint filter bandwidths of 1 Hz, 1.5 Hz, and 0.9 Hz
 - The objective is exceeded for bandwidths of 0.5 Hz, 0.6 Hz, 0.7 Hz, and 0.8 Hz
- The overall trend of the results is similar to the cases without endpoint filter noise generation, i.e., $\max|dTE_R|$ decreases as bandwidth is decreased from 1.5 Hz
 - However now, in addition to $\max|dTE_R|$ increasing due to the longer time over which incoming information from upstream is incorporated into the time estimate, it also increases due to the larger effect of noise generation as the bandwidth decreases
- For the cases here, $\max|dTE_R|$ increases from 400.9 ns to 927.5 ns as endpoint filter bandwidth decreases from 1.5 Hz to 0.5 Hz
 - However, $\max|dTE_R|$ remains below 500 ns for bandwidths in the range 0.9 Hz to 1.5 Hz
 - Note that these results are for discrete values of bandwidth; the actual bandwidth range for which $\max|dTE_R|$ is less than 500 ns likely extends from slightly less than 0.9 Hz to somewhat greater than 1.5 Hz

Discussion of $\max|dTE_R|$ Results for Cases with Endpoint Filter Noise Generation - 2

- As indicated earlier, the maximum Sync interval of 0.131 s corresponds to a minimum Sync rate of $1/(0.131 \text{ s}) = 7.634 \text{ Hz}$. The ratio of this to the 1.0 Hz bandwidth, i.e., the upper end of the range specified in Table 11 of [11], is 7.634. This is less than the 10:1 rule of thumb, but exceeds the theoretical limit of stability for one common PLL implementation. However, the ratio of this to the minimum bandwidth of 0.7 Hz is 10.91, which is greater than the 10:1 rule of thumb
 - Therefore, the endpoint filter bandwidth range for which the 10:1 rule of thumb is met (0.7 Hz to 0.7634 Hz) at least partially covers the range for which the $\max|dTE_R|$ objective is met (0.7 Hz to 1.0 Hz). The theoretical limit of π :1 is met for the entire 0.7 Hz to 1.0 Hz range.
- If the upper end of the bandwidth range of Table 11 of [11] were extended to 1.5 Hz, the ratio of minimum Sync rate to maximum bandwidth would be $7.634 \text{ Hz}/1.5 \text{ Hz} = 5.089$. This is smaller than the ratio for 1.0 Hz bandwidth, but still exceeds the π :1 theoretical limit

Conclusion - 1

- The revised simulation results (compared to the results in [13]) indicate that the $\max|dTE_R|$ objective of 500 ns can be met, under the assumptions described in slides 3 – 5 and 10 – 24 of this presentation, for endpoint filter bandwidths in the range 0.9 Hz to 1.5 Hz.
- These assumptions are contained in [11], either as normative requirements or in the Informative Annex D
 - In particular, the drift tracking and compensation algorithms used here and describe in [1] are also described in Annex D of [11] as an example of algorithms that can be used to meet the $\max|dTE_R|$ objective
- Therefore, it can be stated as a conclusion:
 - Based on the simulation results here, the $\max|dTE_R|$ objective of 500 ns is met for endpoint filter bandwidths in the range 0.9 Hz to 1.5 Hz

Conclusion - 2

- ❑ The current endpoint filter (clock control system) bandwidth requirement in Table 10 of IEC/IEEE 60802/D2.4, Table 11 [11] is a maximum of 1.0 Hz and a minimum of 0.7 Hz
- ❑ Based on the simulation results here, the minimum bandwidth requirement should be increased to:
 - **Minimum Bandwidth (Hz): 0,9 Hz**
- ❑ The maximum bandwidth requirement can remain at 1.0 Hz
 - Alternatively, if desired, the maximum bandwidth requirement could be increased to 1.5 Hz
 - If this is done, there would be less margin relative to the stability limit for the common PLL implementation referred to earlier and described in [8] and [9]. However, in any case it is the responsibility of the implementer to ensure that the endpoint filter (clock control system) design is stable for all conditions

Thank you

References - 1

- [1] David McCall, *60802 Time Sync – Monte Carlo and Time Series Simulation Configuration Including NRR and RR Drift Tracking & Error Compensation*, Version 3, IEC/IEEE 60802 presentation, June 2023, (available at <https://www.ieee802.org/1/files/public/docs2023/60802-McCall-Time-Sync-Simulation-Configuration-NRR-RR-Algorithms-0623-v03.pdf>)
- [2] David McCall, *60802 Time Sync – Monte Carlo Simulations with RR & NRR Drift Tracking and Compensation – Results Part 2*, Version 1, IEC/IEEE 60802 presentation, July 2023, (available at <https://www.ieee802.org/1/files/public/docs2023/60802-McCall-Monte-Carlo-Sim-with-RR-NRR-Drift-Tracking-Comp-Results-Part-2-0723-v02.pdf>)
- [3] David McCall, *IEC/IEEE 60802 Contribution – Time Sync Informative Annex*, Version 3, IEC/IEEE 60802 presentation, August 2023 (available at <https://www.ieee802.org/1/files/public/docs2023/60802-McCall-Time-Sync-Informative-Annex-0823-v03.pdf>)

References - 1

- [4] Geoffrey M. Garner, New Simulation results for Base Case and Case 1 of the Time Sync Breakout Held during the IEC/IEEE 60802 Ad Hoc Session, Revision 2, IEC/IEEE 60802 presentation, July 2022 (available at <https://www.ieee802.org/1/files/public/docs2022/60802-garner-new-simul-results-base-case-case-1-of-June2022-ad-hoc-0722-v02.pdf>)
- [5] Geoffrey M. Garner, *Phase and Frequency Offset, and Frequency Drift Rate Time History Plots Based on New Frequency Stability Data*, IEC/IEEE 60802 presentation, March 8, 2021 call (available at <https://www.ieee802.org/1/files/public/docs2021/60802-garner-temp-freqoffset-plots-based-on-new-freq-stabil-data-0321-v00.pdf>)
- [6] Chris McCormick, *Crystal Fundamentals & State of the Industry*, IEC/IEEE 60802 presentation, February 22, 2021 call (available at <https://www.ieee802.org/1/files/public/docs2021/60802-McCormick-Osc-Stability-0221-v01.pdf>)
- [7] ITU-T Rec. G.8251, *The control of jitter and wander within the optical transport network*, ITU-T, Geneva, November 2022

References - 2

- [8] ITU-T Series G Supplement 65, *Simulations of transport of time over packet networks*, ITU-T, Geneva, October 2018
- [9] John Rogers, Calvin Plett, Foster Dai, *Integrated Circuit Design for High-Speed Frequency Synthesis*, Artech House, 2006.
- [10] Geoffrey M. Garner, *New 60802 Time Domain Simulation Results for Cases with Drift Tracking Algorithms and PLL Noise Generation, Revision 1*, IEC/IEEE 60802 presentation, September 8, 2023 (Revision 0), October 13, 2023 (Revision 1) (available at <https://www.ieee802.org/1/files/public/docs2023/60802-garner-new-time-domain-simul-results-with-drift-tracking-algorithms-and-PLL-noise-generation.pdf>)
- [11] IEC/IEEE 60802 Time Sensitive Networking Profile for Industrial Automation, Draft D2.4, October 2023.
- [12] David McCall, Figures supplied on March 25, 2024

References - 3

- [13] Geoffrey M. Garner, *New Multiple Replication 60802 Time Domain Simulation Results for Cases with Drift Tracking Algorithms and PLL Noise Generation*, Revision 1, October 20, 2023 (available at <https://www.ieee802.org/1/files/public/docs2023/60802-garner-new-time-domain-simul-results-with-drift-tracking-algorithms-and-PLL-noise-generation-multiple-replic-1023-v01.pdf>)
- [14] Geoffrey M. Garner, *Revised 60802 Error Generation Time Series Simulation Results*, Version 1, April 26, 2024 (available at <https://www.ieee802.org/1/files/public/docs2024/60802-garner-revised-error-generation-time-series-simulation-results-0424-v01.pdf>)
- [15] Geoffrey M. Garner, *Further 60802 Error Generation Time Series Simulation Results*, Version 2, March 11, 2024 (available at <https://www.ieee802.org/1/files/public/docs2024/60802-garner-further-error-generation-time-series-simulation-results-0324-v02.pdf>)